

**APPENDIX G**

**GEOVISION FINAL REPORT (GEOPHYSICAL  
TESTING)**



**TURKEY POINT UNITS 6 & 7  
BOREHOLE GEOPHYSICS**

**BORINGS R-6-1a-A, R-6-1b, R-7-1  
AND R-7-4**

**Report 13331-01 rev 1**

**January 17, 2014**

**TURKEY POINT UNITS 6 & 7  
BOREHOLE GEOPHYSICS**

**BORINGS R-6-1a-A, R-6-1b, R-7-1  
AND R-7-4**

**Report 13331-01 rev 1**

**January 17, 2014**

**Prepared for:**

**Paul C. Rizzo Associates, Inc.  
500 Penn Center Boulevard, Suite 100  
Pittsburg, Pennsylvania 15235  
412-856-9700**

**Rizzo Project Number 084075**

**Prepared by**

**GEOVision Geophysical Services  
1124 Olympic Drive  
Corona, California 92881  
(951) 549-1234**

## TABLE OF CONTENTS

<b>TABLE OF CONTENTS .....</b>	<b>3</b>
<b>TABLE OF FIGURES .....</b>	<b>4</b>
<b>TABLE OF TABLES.....</b>	<b>4</b>
<b>TABLE OF APPENDICIES.....</b>	<b>5</b>
<b>INTRODUCTION.....</b>	<b>6</b>
<b>SCOPE OF WORK .....</b>	<b>6</b>
<b>INSTRUMENTATION .....</b>	<b>8</b>
SUSPENSION VELOCITY INSTRUMENTATION.....	8
ACOUSTIC TELEVIEWER / BORING DEVIATION INSTRUMENTATION.....	10
CALIPER / NATURAL GAMMA INSTRUMENTATION.....	13
<b>MEASUREMENT PROCEDURES .....</b>	<b>15</b>
SUSPENSION VELOCITY MEASUREMENT PROCEDURES.....	15
ACOUSTIC TELEVIEWER / BORING DEVIATION MEASUREMENT PROCEDURES.....	16
CALIPER / NATURAL GAMMA MEASUREMENT PROCEDURES.....	17
<b>DATA ANALYSIS .....</b>	<b>19</b>
SUSPENSION VELOCITY ANALYSIS .....	19
ACOUSTIC TELEVIEWER / BORING DEVIATION ANALYSIS .....	21
CALIPER / NATURAL GAMMA ANALYSIS .....	22
<b>RESULTS .....</b>	<b>23</b>
SUSPENSION VELOCITY RESULTS.....	23
ACOUSTIC TELEVIEWER / BORING DEVIATION RESULTS .....	24
CALIPER / NATURAL GAMMA RESULTS.....	24
<b>SUMMARY.....</b>	<b>25</b>
DISCUSSION OF SUSPENSION VELOCITY RESULTS.....	25
DISCUSSION OF ACOUSTIC TELEVIEWER / BORING DEVIATION RESULTS.....	26
DISCUSSION OF CALIPER / NATURAL GAMMA RESULTS.....	26
QUALITY ASSURANCE .....	27
SUSPENSION VELOCITY DATA RELIABILITY.....	27

## Table of Figures

Figure 1: Concept illustration of Suspension P S logging system .....	30
Figure 2: Example of filtered (1400 Hz lowpass) suspension record .....	31
Figure 3. Example of unfiltered suspension record .....	32
Figure 4: Concept illustration of televiewer probe.....	33
Figure 5. Boring R-6-1a-A, Up Deviation Projection (dimensions in feet) .....	34
Figure 6: Boring R-6-1b Suspension R1-R2 P- and $S_H$ -wave velocities.....	35
Figure 7. Boring R-6-1b, Up Deviation Projection (dimensions in feet) .....	44
Figure 8. Boring R-6-1b, Caliper and Natural gamma logs .....	45
Figure 9: Boring R-7-1, Suspension R1-R2 P- and $S_H$ -wave velocities.....	46
Figure 10. Boring R-7-1, Up Deviation Projection (dimensions in feet) .....	55
Figure 11. Boring R-7-1, Caliper and Natural gamma logs .....	56
Figure 12. Boring R-7-4, Up Deviation Projection (dimensions in feet) .....	57

## Table of Tables

Table 1. Boring locations and logging dates.....	28
Table 2. Logging dates and depth ranges .....	28
Table 3. Boring Bottom Depths and After Survey Depth Error (ASDE).....	29
Table 4. Boring Deviation Data Summary .....	29
Table 5. Boring R-6-1b, Suspension R1-R2 depths and P- and $S_H$ -wave velocities.....	36
Table 6. Boring R-6-1b, Structure depth, dip azimuth, dip and structure description.....	43
Table 7. Boring R-7-1, Suspension R1-R2 depths and P- and $S_H$ -wave velocities.....	47
Table 8. Boring R-7-1, Structure depth, dip azimuth, dip and structure description.....	54

**TABLE OF APPENDICIES**

<b>APPENDIX A</b>	<b>SUSPENSION VELOCITY MEASUREMENT QUALITY ASSURANCE SUSPENSION SOURCE TO RECEIVER ANALYSIS RESULTS.....</b>	<b>58</b>
<b>APPENDIX B</b>	<b>ACOUSTIC TELEVIEWER BASED CALIPER LOGS.....</b>	<b>75</b>
<b>APPENDIX C</b>	<b>ACOUSTIC TELEVIEWER FEATURES LOGS.....</b>	<b>202</b>
<b>APPENDIX D</b>	<b>CALIPER AND NATURAL GAMMA LOGS.....</b>	<b>329</b>
<b>APPENDIX E</b>	<b>GEOPHYSICAL LOGGING SYSTEMS - NIST TRACEABLE CALIBRATION PROCEDURES AND CALIBRATION RECORDS.....</b>	<b>356</b>
<b>APPENDIX F</b>	<b>BORING GEOPHYSICAL LOGGING FIELD DATA LOGS.....</b>	<b>359</b>
<b>APPENDIX G</b>	<b>BORING GEOPHYSICAL LOGGING FIELD MEASUREMENT PROCEDURES.....</b>	<b>398</b>

## INTRODUCTION

Boring geophysical measurements were collected in two cased and two uncased borings located at the Florida Power and Light (FPL) Turkey Point Units 6 & 7 site, located near Florida City, Florida. Geophysical data acquisition was performed between October 14 and 16, 2013 by Charles Carter of **GEOVision**. Data analysis was performed by Charles Carter, Victor Gonzalez and Emily Feldman and reviewed by Robert Steller of **GEOVision**. Report preparation was performed by Emily Feldman and reviewed by John Diehl of **GEOVision**. The work was performed under subcontract with Paul C. Rizzo Associates, Inc. (Rizzo) with M. Melih Demirkan serving as the point of contact for Rizzo.

This report describes the field measurements, data analysis, and results of this work.

## SCOPE OF WORK

This report presents the results of boring geophysical measurements collected between October 14 and 16, 2013, in four borings, as detailed in Table 1. The purpose of these studies was to supplement stratigraphic information obtained during Rizzo's soil and rock sampling program and to acquire shear wave velocities and compressional wave velocities as a function of depth, as a component of the Turkey Point Units 6 & 7 site investigation.

The OYO Suspension PS Logging System (Suspension System) was used to obtain in-situ horizontal shear ( $S_H$ ) and compressional (P) wave velocity measurements in two borings at 1.6 foot intervals. Measurements followed **GEOVision** Procedure for P-S Suspension Seismic Velocity Logging, revision 1.5. This procedure was supplied and approved in advance of the work and is reproduced in Appendix G. The acquired data was analyzed and a profile of velocity versus depth was produced for both compressional and horizontally polarized shear waves.

A detailed reference for the suspension PS velocity measurement techniques used in this study is:

Guidelines for Determining Design Basis Ground Motions, Report TR-102293,  
Electric Power Research Institute, Palo Alto, California, November 1993,  
Sections 7 and 8.

The Robertson High Resolution Acoustic Televiwer (HiRAT) was used to collect deviation data at 0.04 foot intervals in all borings and acoustic televiwer images at 0.004 foot intervals in the two uncased borings. Measurements followed the **GEOVision** HiRAT Field Procedure, revision 2.0. This procedure was supplied and approved in advance of the work and is reproduced in Appendix G. The acquired data was analyzed and a profile of boring deviation versus depth was produced for each boring in both downward and upward logging directions. An acoustic image of the two uncased borings, with 4 arm caliper dimensions superimposed was produced for the two uncased borings. In addition, the boring images were analyzed and planar features such as bedding planes and fractures were identified for dip and azimuth processing,

The Robertson 3ACS mechanical caliper probe (CAL) was used to collect boring diameter and natural gamma data at 0.05 foot intervals in the two uncased borings to aid in identification of stratigraphic transitions. Measurement procedures followed these ASTM standards:

- ASTM D5753-05 (Reapproved 2010), “Planning and Conducting Borehole Geophysical Logging”
- ASTM D6167-11, “Conducting Borehole Geophysical Logging: Mechanical Caliper”
- ASTM D6274-10, “Conducting Borehole Geophysical Logging – Gamma”

## INSTRUMENTATION

### Suspension Velocity Instrumentation

Suspension velocity measurements were performed using the Suspension PS logging system serial number 160024, manufactured by OYO Corporation, and their subsidiary, Robertson Geologging. This system directly determines the average velocity of a 3.3 foot high segment of the soil column surrounding the boring of interest by measuring the elapsed time between arrivals of a wave propagating upward through the soil column. The receivers that detect the wave, and the source that generates the wave, are moved as a unit in the boring producing relatively constant amplitude signals at all depths.

The suspension system probe consists of a combined reversible polarity solenoid horizontal shear-wave source ( $S_H$ ) and compressional-wave source (P), joined to two biaxial receivers by a flexible isolation cylinder, as shown in Figure 1. The separation of the two receivers is 3.28 feet, allowing average wave velocity in the region between the receivers to be determined by inversion of the wave travel time between the two receivers. The total length of the probe as used in these surveys is 21 feet, with the center point of the receiver pair 12.5 feet above the bottom end of the probe.

The probe receives control signals from, and sends the digitized receiver signals to, instrumentation on the surface via an armored multi-conductor cable. The cable is wound onto the drum of a winch and is used to support the probe. Cable travel is measured to provide probe depth data, using a sheave of known circumference fitted with a digital rotary encoder.

The entire probe is suspended in the boring by the cable, therefore, source motion is not coupled directly to the boring walls; rather, the source motion creates a horizontally propagating impulsive pressure wave in the fluid filling the boring and surrounding the source. This pressure wave is converted to P and  $S_H$ -waves in the surrounding soil and rock as it passes through the casing and grout annulus and impinges upon the wall of the boring. These waves propagate

through the soil and rock surrounding the boring, in turn causing a pressure wave to be generated in the fluid surrounding the receivers as the soil waves pass their location. Separation of the P and  $S_H$ -waves at the receivers is performed using the following steps:

1. Orientation of the horizontal receivers is maintained parallel to the axis of the source, maximizing the amplitude of the recorded  $S_H$  -wave signals.
2. At each depth,  $S_H$ -wave signals are recorded with the source actuated in opposite directions, producing  $S_H$ -wave signals of opposite polarity, providing a characteristic  $S_H$ -wave signature distinct from the P-wave signal.
3. The 6.3 foot separation of source and receiver 1 permits the P-wave signal to pass and damp significantly before the slower  $S_H$ -wave signal arrives at the receiver. In faster soils or rock, the isolation cylinder is extended to allow greater separation of the P- and  $S_H$ -wave signals.
4. In saturated soils, the received P-wave signal is typically of much higher frequency than the received  $S_H$ -wave signal, permitting additional separation of the two signals by low pass filtering.
5. Direct arrival of the original pressure pulse in the fluid is not detected at the receivers because the wavelength of the pressure pulse in fluid is significantly greater than the dimension of the fluid annulus surrounding the probe (meter versus centimeter scale), preventing significant energy transmission through the fluid medium.

In operation, a distinct, repeatable pattern of impulses is generated at each depth as follows:

1. The source is fired in one direction producing dominantly horizontal shear with some vertical compression, and the signals from the horizontal receivers situated parallel to the axis of motion of the source are recorded.
2. The source is fired again in the opposite direction and the horizontal receiver signals are recorded.
3. The source is fired again and the vertical receiver signals are recorded. The repeated source pattern facilitates the picking of the P and  $S_H$ -wave arrivals; reversal of the source changes the polarity of the  $S_H$ -wave pattern but not the P-wave pattern.

The data from each receiver during each source activation is recorded as a different channel on the recording system. The Suspension PS system has six channels (two simultaneous recording channels), each with a 1024 sample record. The recorded data are displayed as six channels with a common time scale. Data are stored on disk for further processing. Up to 8 sampling sequences can be summed to improve the signal to noise ratio of the signals.

Review of the displayed data on the recorder or computer screen allows the operator to set the gains, delay time, pulse length (energy), sample rate, and summing number to optimize the quality of the data before recording. Verification of the calibration of the Suspension PS digital recorder is performed every twelve months using a NIST traceable frequency source and counter, as outlined in Appendix E.

### **Acoustic Televierer / Boring Deviation Instrumentation**

An acoustic image and/or boring deviation data were collected using a High Resolution Acoustic Televierer probe (HiRAT), serial number 6641, manufactured by Robertson Geologging, Ltd. A concept illustration of the HIRAT probe is shown in Figure 4.

In this application, this probe is useful in the following studies:

- Measurement of boring inclination and deviation from vertical
- Determination of need to correct soil and geophysical log depths to true vertical depths
- Acoustic imaging of the boring wall to identify fractures, dikes, and weathered zones, and determine dip and azimuth of these features

The probe receives control signals from, and sends the digitized measurement values to, a Robertson Micrologger II on the surface via an armored 4 conductor cable. The cable is wound onto the drum of a winch and is used to support the probe. Cable travel is measured to provide probe depth data, using a sheave of known circumference fitted with a digital rotary encoder.

The probe and depth data are transmitted by USB link from the Micrologger unit to a laptop computer where it is displayed and stored on hard disk.

This system produces images of the boring wall based upon the amplitude and travel time of an ultrasonic beam reflected from the formation wall. The ultrasonic energy is generated by a piezoelectric transducer at a frequency of 1.4 MHz. A periodic acoustic energy wave is emitted by the transducer and travels through the acoustic head and boring fluid until it reaches the interface between the boring fluid and the boring wall. Here a portion of the energy is reflected back to the transducer, the remainder continuing into the formation. By careful time sequencing, the piezoelectric transducer acts as both the transmitter of the ultrasonic pulse and receiver of the reflected wave. The travel time of the energy wave is the period between transmission of the source energy pulse and the return of the reflected wave measured at the point of maximum wave amplitude. The magnitude of the wave energy is measured in dB, a unitless ratio of the detected echo wave amplitude divided by the amplitude of the transmitted wave. The strength of the reflected signal depends primarily upon the impedance contrast of the boring fluid and the boring wall formation. In the limestone sections of these borings, the contrast between the fluid filling the boring and the rock formation provides imaging of numerous small solution cavities, as well as areas where weathered limestone has been eroded by the drilling process. In the soil portions of these borings, there is little or no image produced due to the irregular surface and large diameter caused by borehole erosion, and the very low acoustic reflectance of the soil.

The acoustic wave propagates along the axis of the probe and then is reflected perpendicular to this axis by a reflector that focuses the beam to a 0.1-inch diameter spot about 2 inches from the central axis of the probe. This reflector is mounted on the shaft of a stepper motor enabling the position of the measurement to be rotated through 360°. Sampling rates of 90, 180 and 360 measured points per revolution are available. During these surveys, data were collected at 360 samples per revolution for imaging the uncased, and at 90 samples per revolution for deviation data in the other two boreholes. It should be noted that during logging the probe is moving in the boring, so that the measured points describe a very fine pitch spiral.

The probe contains a fluxgate magnetometer to monitor magnetic north, and all raw televiewer data are referenced to magnetic north. The processed data is referenced to true north, using a declination of 6.16 degrees west for this site and dates, obtained from the NOAA declination web site (<http://www.ngdc.noaa.gov/geomag-web/#declination>). Also, a three-axis accelerometer is enclosed in the probe, and boring deviation data are recorded during the logging runs, to permit correction of structure dip angle from apparent dip, referenced to boring axis, to true dip (referenced to a vertical axis) in non-vertical borings.

The data are presented on a computer screen for operator review during the logging run, and stored on hard disk for later processing.

## Caliper / Natural Gamma Instrumentation

Caliper and natural gamma data were collected using a Model 3ACS 3-leg caliper probe, serial number 5368, manufactured by Robertson Geologging, Ltd. With the short arm configuration used in these surveys, the probe permitted measurement of boring diameters between 1.6 and 16 inches. With this tool, caliper measurements were collected concurrent with measurement of natural gamma emission from the boring walls. The probe was 6.82 feet long, and 1.5 inches in diameter.

This probe is useful in the following studies:

- Measurement of boring diameter and volume
- Location of hard and soft formations
- Location of fissures, caving, pinching and casing damage
- Bed boundary identification
- Strata correlation between borings

The probe receives control signals from, and sends the digitized measurement values to, a Robertson Micrologger II on the surface via an armored 4 conductor cable. The cable is wound onto the drum of a winch and is used to support the probe. Cable travel is measured to provide probe depth data, using a sheave of known circumference fitted with a digital rotary encoder. The probe and depth data are transmitted by USB link from the Micrologger unit to a laptop computer where it is displayed and stored on hard disk.

The caliper consists of three arms, each with a toothed quadrant at their base, pivoted in the lower probe body. A toothed rack engages with each quadrant, thus constraining the arms to move together. Linear movement of the rack is converted to opening and closing of the arms. Springs hold the arms open in the operating position. A motor drive is provided to retract the arms, allowing the probe to be lowered into the boring. The rack is coupled to a potentiometer which converts movement into a voltage sensed by the probe's microprocessor.

Natural gamma measurements rely upon small quantities of radioactive material contained in all soil and rocks to emit gamma radiation as they decay. Trace amounts of Uranium and Thorium are present in a few minerals, where potassium-bearing minerals such as feldspar, mica and clays will include traces of a radioactive isotope of Potassium. These emit gamma radiation as they decay with an extremely long half-life. This radiation is detected by scintillation - the production of a tiny flash of light when gamma rays strike a crystal of sodium iodide. The light is converted into an electrical pulse by a photomultiplier tube. Pulses above a threshold value of 60 KeV are counted by the probe's microprocessor. The measurement is useful because the radioactive elements are concentrated in certain rock types e.g. clay or shale, and depleted in others e.g. sandstone or coal.

## MEASUREMENT PROCEDURES

### Suspension Velocity Measurement Procedures

Measurements followed the *GEOVision* Procedure for P-S Suspension Seismic Velocity Logging, revision 1.5, as presented in Appendix G. These procedures were supplied and approved in advance of the work. Two borings were logged filled fresh water mud. Prior to each logging run, the probe was positioned with the top of the probe at the top of the surface casing, and the electronic depth counter was set to the distance between the mid-point of the receiver and the top of the probe, minus the height of any casing stick-up, as verified with a tape measure, and recorded on the field logs. The probe was lowered to the bottom of the boring, and then returned to the bottom of the surface casing, stopping at 1.64 foot intervals to collect data, as summarized in Table 2.

At each measurement depth the measurement sequence of two opposite horizontal records and one vertical record was performed, and the gains were adjusted as required. The data from each depth were viewed on the computer display, checked to verify acceptable signal levels, and recorded on disk before moving to the next depth.

Upon completion of the measurements, the probe zero depth indication at the depth reference point was verified prior to removal from the boring, and the after survey depth error (ASDE) was calculated and recorded on the field logs, as summarized in Table 3. Field data were backed up to USB drive each day upon completion of data acquisition.

## **Acoustic Televiwer / Boring Deviation Measurement Procedures**

Two uncased borings were logged while filled with water for acoustic televiwer data and two borings were logged dry and cased for deviation data only. Measurement procedures followed **GEO***Vision* HI-RAT procedure revision 2.0. This procedure was supplied and approved in advance of the work and is reproduced in Appendix G. Prior to use, the probe tiltmeter and compass functions were checked by comparison with a Brunton surveyors' compass, and the results recorded on the field logs, as reproduced in Appendix F.

In each boring, the HiRAT probe was positioned with the top of the probe at the top of the casing, and the electronic depth counter was set to the specified length of the probe, minus the height of the casing stick-up, as verified with a tape measure, and recorded on the field logs. The probe was lowered to the bottom of the boring while collecting a low vertical resolution image. At the bottom of the boring, this image was closed, and a collection of a high vertical resolution image was begun.

Upon completion of the measurements, the probe zero depth indication at the depth reference point was verified prior to removal from the boring, and the after survey depth error (ASDE) was calculated, as summarized in Table 3. The log was reviewed in the field, and all data were backed up to USB drive each day upon completion of data acquisition.

## Caliper / Natural Gamma Measurement Procedures

Two uncased borings were logged, filled with fresh water mud. This probe was not calibrated in the field, as it is used to provide qualitative measurements, not quantitative values, and is used only to assist in picking transitions between stratigraphic units, as described in ASTM D5753-05 (Reapproved 2010), “Planning and Conducting Borehole Geophysical Logging” and ASTM D6167-11 “Conducting Borehole Geophysical Logging – Mechanical Caliper”. Measurements also followed the same ASTM standards.

Prior to and following each logging run, the caliper tool was verified, using an approved three point calibration jig (S/N 201). The three point jig is a circular plate with a series of holes in the top surface into which the tips of the caliper arms fit. This has circles of diameters from 2 to 12 inches. The calibration jig is placed over a bucket with the probe standing upright with its nose section passing through the jig’s central hole. The caliper probe arms are opened under program control, and a log is recorded as the tips of the arms are placed in the holes on the calibration jig and inside the PVC coupling. The measured dimensions, as displayed on the recording computer screen was recorded on the field log sheet, as well as in the digital files, and compared with the calibration jig dimensions. . These functional checks are presented in LAS 2.0 format in the sub-directories of the data package titled Report 13331-02 delivered separately to Rizzo.

If the verification records did not fall within +/- 0.05 inches of the calibration jig values, the caliper tool was re-calibrated using the three point calibration jig and the log repeated. As with the verification, the tips of the caliper arms are placed in the holes marked with the required diameter. During calibration, the value of the current calibration point, as stamped on the jig, is entered via the control computer. The system counts for 15 seconds to make an average of the response. The procedure is repeated for the second and third required openings.

The computation and generation of the calibration coefficient file is entirely automatic. The calibration file is simply the set of coefficients of a quadratic curve which fits the three data points.

Natural gamma was not calibrated in the field, as it is a qualitative measurement, not a quantitative value, and is used only to assist in picking transitions between stratigraphic units, as described in ASTM D6274-10, “Conducting Borehole Geophysical Logging – Gamma”.

Prior to each logging run, the sensor positions were referenced to ground level. This was done by placing the top of the probe at grade, and the electronic depth counter was set to the probe length. These calculations are recorded on the field logs. Offset distances between probe tip and Induction and natural gamma sensors are corrected for in the data acquisition software. The probe was lowered to the bottom of the boring, where data collection was begun. The probe was then returned to the surface at approximately 10.0 feet/minute, collecting data continuously at 0.050 foot spacing, as summarized in Table 2.

Upon completion of the measurements, the probe zero depth indication at the depth reference point was verified prior to removal from the boring, and the after survey depth error (ASDE) was calculated, as summarized in Table 3. Field data were backed up to USB drive each day upon completion of data acquisition.

## DATA ANALYSIS

### Suspension Velocity Analysis

Using the proprietary OYO program PSLOG.EXE version 1.0, included in the data package Report 13331-02 delivered separately to Rizzo, the recorded digital waveforms were analyzed to locate the most prominent first minima, first maxima, or first break on the vertical axis records, indicating the arrival of P-wave energy.

The difference in travel time between receiver 1 and receiver 2 (R1-R2) arrivals was used to calculate the P-wave velocity for that 3.28 feet segment of the soil column. When observable, P-wave arrivals on the horizontal axis records were used to verify the velocities determined from the vertical axis data. The time picks were transferred into a Microsoft Excel<sup>®</sup> template (version 2003 SP2) to complete the velocity calculations based upon the arrival time picks made in PSLOG and actual R1-R2 separation. The PSLOG pick files and the Microsoft Excel<sup>®</sup> analysis files are included in the data package Report 13331-02 delivered separately to Rizzo.

The P-wave velocity over the 6.3 foot interval from source to receiver 1 (S-R1) was also picked using PSLOG, and calculated and plotted in Microsoft Excel<sup>®</sup>, for verification of the velocity derived from the travel time between receivers. In this analysis, the depth values as recorded were increased by 4.8 feet to correspond to the mid-point of the 6.3 foot S-R1 interval. Travel times were obtained by picking the first break of the P-wave signal at receiver 1 and subtracting 0.3 milliseconds, the calculated and experimentally verified delay from source trigger pulse (beginning of record) to source impact. This delay corresponds to the duration of acceleration of the solenoid before impact.

As with the P-wave records, the recorded digital waveforms were analyzed to locate clear  $S_H$ -wave pulses, as indicated by the presence of opposite polarity pulses on each pair of horizontal records. Ideally, the  $S_H$ -wave signals from the 'normal' and 'reverse' source pulses are very nearly inverted images of each other. Digital Fast Fourier Transform – Inverse Fast Fourier

Transform (FFT – IFFT) lowpass filtering was used to remove the higher frequency P-wave signal from the  $S_H$ -wave signal. Different filter cutoffs were used to separate P- and  $S_H$ -waves at different depths, ranging from 600 Hz in the slowest zones to 4000 Hz in the regions of highest velocity. At each depth, the filter frequency was selected to be at least twice the fundamental frequency of the  $S_H$ -wave signal being filtered.

Generally, the first maxima were picked for the 'normal' signals and the first minima for the 'reverse' signals, although other points on the waveform were used if the first pulse was distorted. The absolute arrival time of the 'normal' and 'reverse' signals may vary by +/- 0.2 milliseconds, due to differences in the actuation time of the solenoid source caused by constant mechanical bias in the source or by boring inclination. This variation does not affect the R1-R2 velocity determinations, as the differential time is measured between arrivals of waves created by the same source actuation. The final velocity value is the average of the values obtained from the 'normal' and 'reverse' source actuations.

As with the P-wave data,  $S_H$ -wave velocity calculated from the travel time over the 6.3 foot interval from source to receiver 1 was calculated and plotted for verification of the velocity derived from the travel time between receivers. In this analysis, the depth values were increased by 4.8 foot to correspond to the mid-point of the 6.3 foot S-R1 interval. Travel times were obtained by picking the first break of the  $S_H$ -wave signal at the near receiver and subtracting 0.3 milliseconds, the calculated and experimentally verified delay from the beginning of the record at the source trigger pulse to source impact.

These data and analysis were reviewed by John Diehl as a component of **GEOVision's** in-house data validation program.

Figure 2 shows an example of R1 - R2 measurements on a sample filtered suspension record. In Figure 2, the time difference over the 3.28 foot interval of 1.88 milliseconds for the horizontal signals is equivalent to an  $S_H$ -wave velocity of 1745 feet/second. Whenever possible, time differences were determined from several phase points on the  $S_H$ -waveform records to verify the data obtained from the first arrival of the  $S_H$ -wave pulse. Figure 3 displays the same record

before filtering of the  $S_H$ -waveform record with a 1400 Hz FFT - IFFT digital lowpass filter, illustrating the presence of higher frequency P-wave energy at the beginning of the record, and distortion of the lower frequency  $S_H$ -wave by residual P-wave signal.

### **Acoustic Televiwer / Boring Deviation Analysis**

The acoustic televiwer data were processed using Robertson Geologging RGLDIP™ software, version 6.2. Sinusoidal projections of planar and semi-planar features in the boring walls were interactively picked on the un-wrapped televiwer image, and are presented on the logs as sinusoids superimposed over the televiwer image, as presented in Appendix C. Green corresponds to bedding features and blue indicates fractures. Bedding features at this site are very numerous, and adjacent features are generally of similar dip and azimuth. Representative bedding features were selected, as picking all features would create an overly complex presentation. The sinusoidal projections were processed to calculate apparent dip angle using the nominal borehole diameter for each boring. True dip was calculated, correcting for the inclination of the borings using the recorded data from the accelerometers located in the probe, and presented in arrow format, with true dip indicated by the arrow position across the plot. Azimuth of dip (not strike), is indicated by the direction of the arrow tail, with true north being “up”. These values are presented with the comments to the right of the arrow plots, as dip azimuth followed by dip angle.

The televiwer images were also processed to create a simulated core image of the borings. It must be noted that the simulated core image represents a core that would have the full diameter of the boring, not the diameter of the cores removed during drilling, so that direct comparison between the two is not possible. Also, the unwrapped image is viewed from the perspective of an observer in the center of the boring looking outward. The simulated core image is viewed from the “outside” of the boring looking inward, so there is a reversal of the position of east and west relative to north between the two images.

The televiewer data were also processed to extract the deviation data and produce an ASCII file and plots of boring deviation, as well as a 4-arm caliper log, derived from the acoustic travel time data. No stereonet analysis of the identified features was performed, as there does not appear to be dominant jointing present in the borings.

### **Caliper / Natural Gamma Analysis**

No analysis is required with the caliper or natural gamma data; however depths to identifiable boring features were compared to verify compatible depth readings on all logs. Using ALT WellCAD™ software version 4.3, these data were converted to LAS 2.0 and PDF formats for transmittal to the client.

## RESULTS

### Suspension Velocity Results

Suspension R1-R2 P- and  $S_H$ -wave velocities from borings R-6-1b and R-7-1 are plotted in Figures 6 and 9, respectively. The suspension velocity data presented in these figures are presented in Tables 5 and 7. Depths on all figures and tables are referenced to ground surface. The PSLOG and Microsoft Excel<sup>®</sup> analysis files for each boring are included in the data package Report 13331-02 delivered separately to Rizzo.

P- and  $S_H$ -wave velocity data from R1-R2 analysis and quality assurance analysis of S-R1 data are plotted together in Appendix A as Figures A-1 and A-2 to aid in visual comparison. It should be noted that R1-R2 data are an average velocity over a 3.28 feet segment of the soil column; S-R1 data are an average over 6.3 feet, creating a significant smoothing relative to the R1-R2 plots. S-R1 data are presented in Tables A-1 and A-2, and in the Microsoft Excel<sup>®</sup> analysis files for each boring included in the data package Report 13331-02 delivered separately to Rizzo. The Microsoft Excel<sup>®</sup> analysis files include Poisson's Ratio calculations, tabulated data and plots. The data presented in these reports is marked as rev 1 or above, with rev 0 being the unprocessed data, as collected in the field.

Calibration procedures and records for the suspension PS measurement system are presented in Appendix E, and **GEOVision** standard field log sheets for all borings are reproduced in Appendix F.

The approved **GEOVision** standard field procedures, as provided to Rizzo for approval prior to field work, are reproduced in Appendix G.

## **Acoustic Televiewer / Boring Deviation Results**

Acoustic televiewer amplitude images and acoustic travel-time derived boring radii from borings R-6-1b and R-7-1 are presented in Appendix B. The same logs are included in .PDF formation in the data package Report 13331-02 delivered separately to Rizzo. Fracture and bedding depth, dip and azimuth of dip data are provided on the multi-page log sheets in Appendix C, in Tables 6 and 8 as well as in Microsoft Excel<sup>®</sup> format in the data package Report 13331-02 delivered separately to Rizzo.

Boring deviation data for borings R-6-1a-A, R-6-1b, R-7-1 and R-7-4 in the upward direction are presented graphically in Figures 5, 7, 10 and 12, and summarized in Table 4. Deviation data plots in .PDF format and deviation data at 1.0 foot stations in text format from logging in both directions are presented in the boring specific sub- in the data package Report 13331-02 delivered separately to Rizzo. The data presented in these reports is marked as rev 1 or above, with rev 0 being the unprocessed data, as collected in the field.

## **Caliper / Natural Gamma Results**

Caliper and natural gamma data from boreholes R-6-1b and R-7-1 are presented in combined log plots as single page logs in Figures 8 and 11, as well as multi-page logs in Appendix D. On these plots, the Natural gamma data collected with the caliper probe is displayed as “Natural Gamma” and the caliper as “Borehole Diameter”

LAS 2.0 data and Acrobat files of the plots for each boring are included in the boring specific sub-directories in the data package Report 13331-02 delivered separately to Rizzo. The data presented in these reports is marked as rev 1 or above, with rev 0 being the unprocessed data, as collected in the field.

## SUMMARY

### Discussion of Suspension Velocity Results

Suspension PS velocity data are ideally collected in an uncased fluid filled boring, drilled with rotary mud (rotary wash) methods. Due to the erosion of the borehole walls, data quality was not optimal.

Suspension PS velocity data quality is judged based upon 5 criteria:

1. Consistent data between receiver to receiver (R1 – R2) and source to receiver (S – R1) data.
2. Consistent relationship between P-wave and  $S_H$ -wave (excluding transition to saturated soils)
3. Consistency between data from adjacent depth intervals.
4. Clarity of P-wave and  $S_H$ -wave onset, as well as damping of later oscillations.
5. Consistency of profile between adjacent borings, if available.

These data show good correlation between R1 – R2 and S – R1 data, as well as good correlation between P-wave and  $S_H$ -wave velocities. P-wave and  $S_H$ -wave onsets are generally clear, and later oscillations are well damped. The profiles are similar, with slight variation of depths and peak velocities of harder layers. These profiles are similar to data collected at this site during previous projects.

## **Discussion of Acoustic Televiwer / Boring Deviation Results**

The acoustic televiwer image quality in the two uncased borings was poor due to the quality of the borehole walls. Significant voids exist above 150 feet in both borings, with widths of 2 to 4 feet in boring R-7-1 up to 10 feet in R-6-1b, where the mechanical caliper was allowed to open to its full 14 inch diameter. Numerous smaller voids and eroded zones are present in the limestone rock in the top 150 feet of the borings, with apertures of 1-2 feet the and the calipers opening to 8 to 10 inches wide. Below the limestone, the borings show degradation of image quality and derived caliper stability due to sediment in the boring fluid and erosion of boring walls. Location of softer zones on the televiwer logs and increases in boring diameter correspond well with decreases in suspension PS velocity values.

The two uncased borings were inclined at less than one degree from vertical, and the maximum error in depth value resulting from this deviation was 0.23 feet in 465 feet, or less than 0.04 percent, as presented in Table 4. This error is less than depth errors from other sources, and, for reference, is substantially less than the 0.4% error from after survey depth error (ASDE) permitted under ASTM D6167-11 “Conducting Borehole Geophysical Logging – Mechanical Caliper” Section 9.15.4. No adjustment of log depths is indicated. The two cased borings were were inclined at 14 to 16 degrees from vertical and have a maximum error in depth value expectedly higher, of 4.6 feet in 122.5 feet or about 3.8%. However these borings were only logged to extract borehole deviation data, making their depth error inconsequential.

## **Discussion of Caliper / Natural Gamma Results**

Caliper and natural gamma data were collected for the entire depth of each uncased boring. The caliper logs for these borings generally show a diameter of less than 5 inches, however there are numerous areas in which the diameter was eroded out to more than 14 inches. There may be differences in the boring diameters at the same depth from different logging runs due to reaming of the boring, or erosion by the drilling fluid between logging runs.

## Quality Assurance

These boring geophysical measurements were performed using industry-standard or better methods for measurements and analyses. All work was performed under Rizzo quality assurance procedures, which include:

- Use of NIST-traceable calibrations, where applicable, for field and laboratory instrumentation
- Use of standard field data logs
- Use of independent verification of velocity data by comparison of receiver-to-receiver and source-to-receiver velocities
- Independent review of calculations and results by a registered professional engineer, geologist, or geophysicist.
- Field surveillance by Rizzo Quality, Health, Safety and Environmental (QHSE) Staff.

## Suspension Velocity Data Reliability

P- and  $S_H$ -wave velocity measurement using the Suspension Method gives average velocities over a 3.28 feet interval of depth. This high resolution results in the scatter of values shown in the graphs. Individual R1-R2 measurements have an estimated precision of +/- 5%. Standardized field procedures and quality assurance checks contribute to the reliability of these data.

Table 1. Boring locations and logging dates

BORING DESIGNATION	DATES LOGGED	COORDINATES (FEET) <sup>(1)</sup>		ELEVATION <sup>(1)</sup> (FEET)
		NORTHING	EASTING	
R-6-1a-A	10/16/2013	397112.22	876590.79	-0.09
R-6-1b	10/14-16/2013	396966.10	876609.04	-0.03
R-7-1	10/15-16/2013	396976.23	875797.30	0.22
R-7-4	10/15/2013	396958.51	875605.22	-0.53

(1)

Provided by Rizzo, email 12/5/2013. Coordinates NAD83, Elevations NAVD88

Table 2. Logging dates and depth ranges

BORING NUMBER	TOOL AND RUN NUMBER	DEPTH RANGE (FEET)	CASED OR UNCASED	SAMPLE INTERVAL (FEET)	DATE LOGGED
R-6-1a-A	DEVIATION DOWN 01	3.6 – 106.5	CASED	0.04	10/16/2013
R-6-1a-A	DEVIATION UP01	106.1 – 3.0	CASED	0.04	10/16/2013
R-6-1b	ACOUSTIC TV DOWN 01	3.2 – 464	UNCASED	0.04	10/14/2013
R-6-1b	ACOUSTIC TV UP01	463.8 – 109	UNCASED	0.004	10/14/2013
R-6-1b	SUSPENSION PS DOWN01	111.55 – 449.48	UNCASED	1.6	10/14/2013
R-6-1b	CALIPER/GAMMA UP01	455.7 – 99.65	UNCASED	0.05	10/15/2013
R-6-1b	ACOUSTIC TV DOWN02	1.9 – 113.5	UNCASED	0.04	10/16/2013
R-6-1b	ACOUSTIC TV UP02	113.5 – 1.6	UNCASED	0.004	10/16/2013
R-6-1b	SUSPENSION PS DOWN02	6.56 – 114.83	UNCASED	1.6	10/16/2013
R-6-1b	CALIPER/GAMMA UP02	116.7 – 3.35	UNCASED	0.05	10/16/2013
R-7-1	ACOUSTIC TV DOWN 01	4.3 – 317.8	UNCASED	0.04	10/15/2013
R-7-1	ACOUSTIC TV UP01	313.2 – 188.5	UNCASED	0.004	10/15/2013
R-7-1	ACOUSTIC TV DOWN02	252 – 454	UNCASED	0.04	10/15/2013
R-7-1	ACOUSTIC TV UP02	453.8 – 284.1	UNCASED	0.004	10/15/2013
R-7-1	SUSPENSION PS DOWN01	191.93 – 441.27	UNCASED	1.6	10/15/2013
R-7-1	CALIPER/GAMMA UP01	450.25 – 179.9	UNCASED	0.05	10/15/2013
R-7-1	ACOUSTIC TV DOWN03	2.5 – 70.5	UNCASED	0.04	10/16/2013
R-7-1	ACOUSTIC TV DOWN04	2.5 – 196.5	UNCASED	0.04	10/16/2013
R-7-1	ACOUSTIC TV UP03	196.5 – 2.4	UNCASED	0.004	10/16/2013
R-7-1	SUSPENSION PS DOWN02	6.56 – 187.01	UNCASED	1.6	10/16/2013
R-7-1	CALIPER/GAMMA UP02	191.75 – 2.5	UNCASED	0.05	10/16/2013
R-7-4	DEVIATION DOWN 01	4.0 – 122.0	CASED	0.04	10/15/2013
R-7-4	DEVIATION UP01	122.1 – 4.0	CASED	0.004	10/15/2013

Table 3. Boring Bottom Depths and After Survey Depth Error (ASDE)

BORING NUMBER	TOOL AND RUN NUMBER	TOOL HIT BOTTOM DEPTH (FEET)	DRILLER DEPTH (FEET)	STARTING DEPTH REF. (FEET)	ENDING DEPTH REF. (FEET)	ASDE (FEET)
R-6-1a-A	DEVIATION DOWN/UP01	-	120	3.55	3.54	0.01
R-6-1b	ACOUSTIC TV DOWN/UP01	-	464	3.11	2.83	0.28
R-6-1b	SUSPENSION PS DOWN01	-	464	6.59	6.43	0.16
R-6-1b	CALIPER/GAMMA UP01	-	464	5.21	3.95	1.26
R-6-1b	ACOUSTIC TV DOWN/UP02	-	464	1.61	1.58	0.03
R-6-1b	SUSPENSION PS DOWN02	-	464	6.59	6.53	0.06
R-6-1b	CALIPER/GAMMA UP02	-	464	5.21	5.20	0.01
R-7-1	ACOUSTIC TV DOWN/UP01	-	455	3.39	2.6	0.93
R-7-1	ACOUSTIC TV DOWN/UP02	-	455	3.39	3.16	0.23
R-7-1	SUSPENSION PS DOWN01	455	455	6.86	6.49	0.37
R-7-1	CALIPER/GAMMA UP01	-	455	5.49	5.35	0.14
R-7-1	ACOUSTIC TV DOWN03	-	455	2.46	2.45	0.01
R-7-1	ACOUSTIC TV DOWN04/UP03	-	455	2.46	2.35	0.11
R-7-1	SUSPENSION PS DOWN02	200	455	6.86	6.66	0.20
R-7-1	CALIPER/GAMMA UP02	-	455	5.49	5.40	0.09
R-7-4	DEVIATION DOWN/UP01	-	120	3.97	3.92	0.05

- PROBE DID NOT TOUCH BOTTOM OF BORING

Table 4. Boring Deviation Data Summary

BORING DESIGNATION / DIRECTION	MEAN DEVIATION AND AZIMUTH (DEGREES TN)	SURVEY DEPTH (FEET)	VERTICAL DEPTH (FEET)	DEPTH ERROR (FEET)	HORIZONTAL OFFSET (FEET)
R-6-1a-A DOWN	14.2 – N313	106.84	103.54	3.30	26.27
R-6-1a-A UP	14.1 – N312	106.28	103.06	3.22	25.89
R-6-1b DOWN	0.4 – N21	464.85	464.62	0.23	3.47
R-6-1b UP	0.3 – N11	464.29	464.21	0.08	2.05
R-7-1 DOWN	0.8 – N107	453.87	453.75	0.12	6.50
R-7-1 UP	0.8 – N95	454.00	453.88	0.12	6.57
R-7-4 DOWN	15.8 – N96	122.48	117.86	4.62	33.29
R-7-4 UP	15.8 – N96	122.45	117.83	4.62	33.30

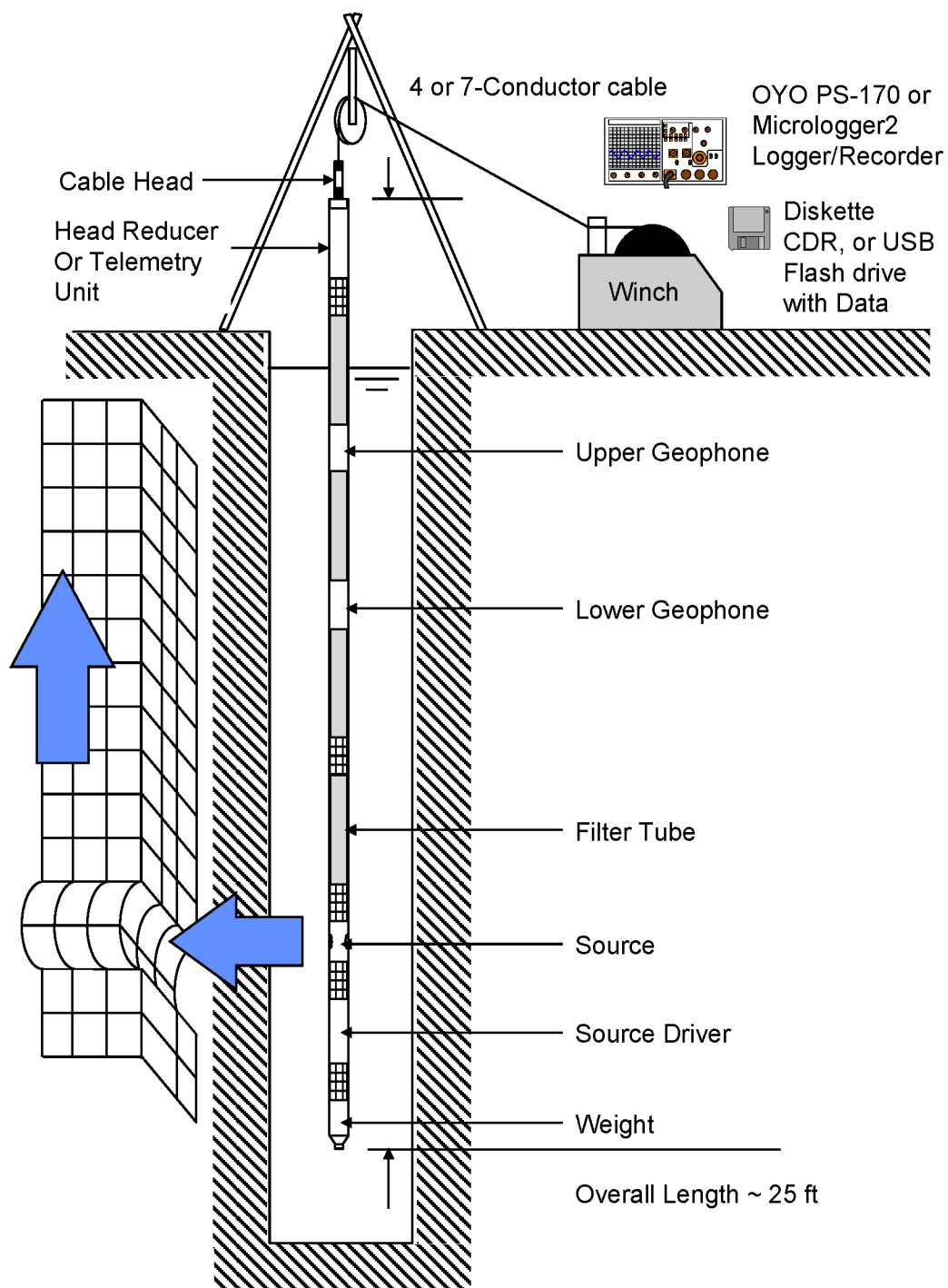


Figure 1: Concept illustration of Suspension P S logging system

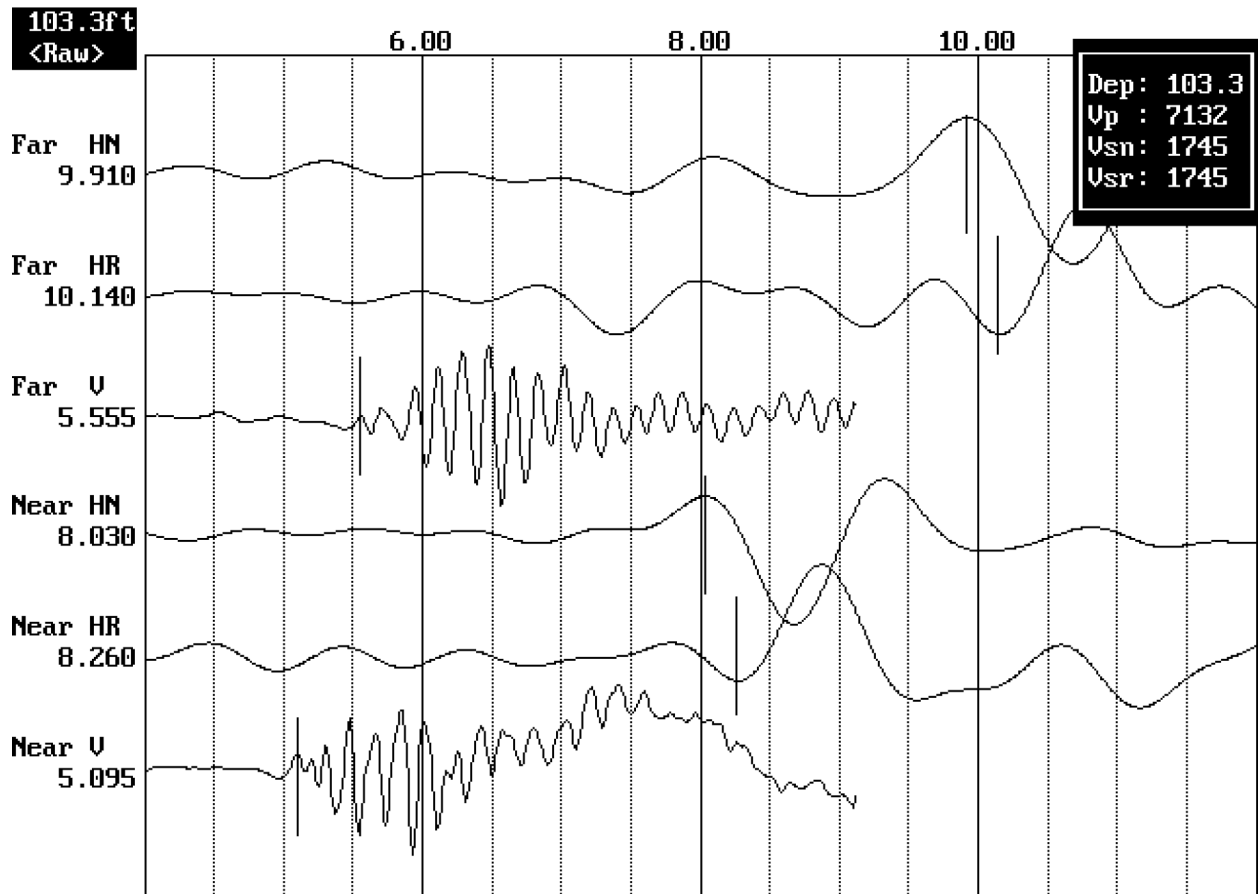


Figure 2: Example of filtered (1400 Hz lowpass) suspension record

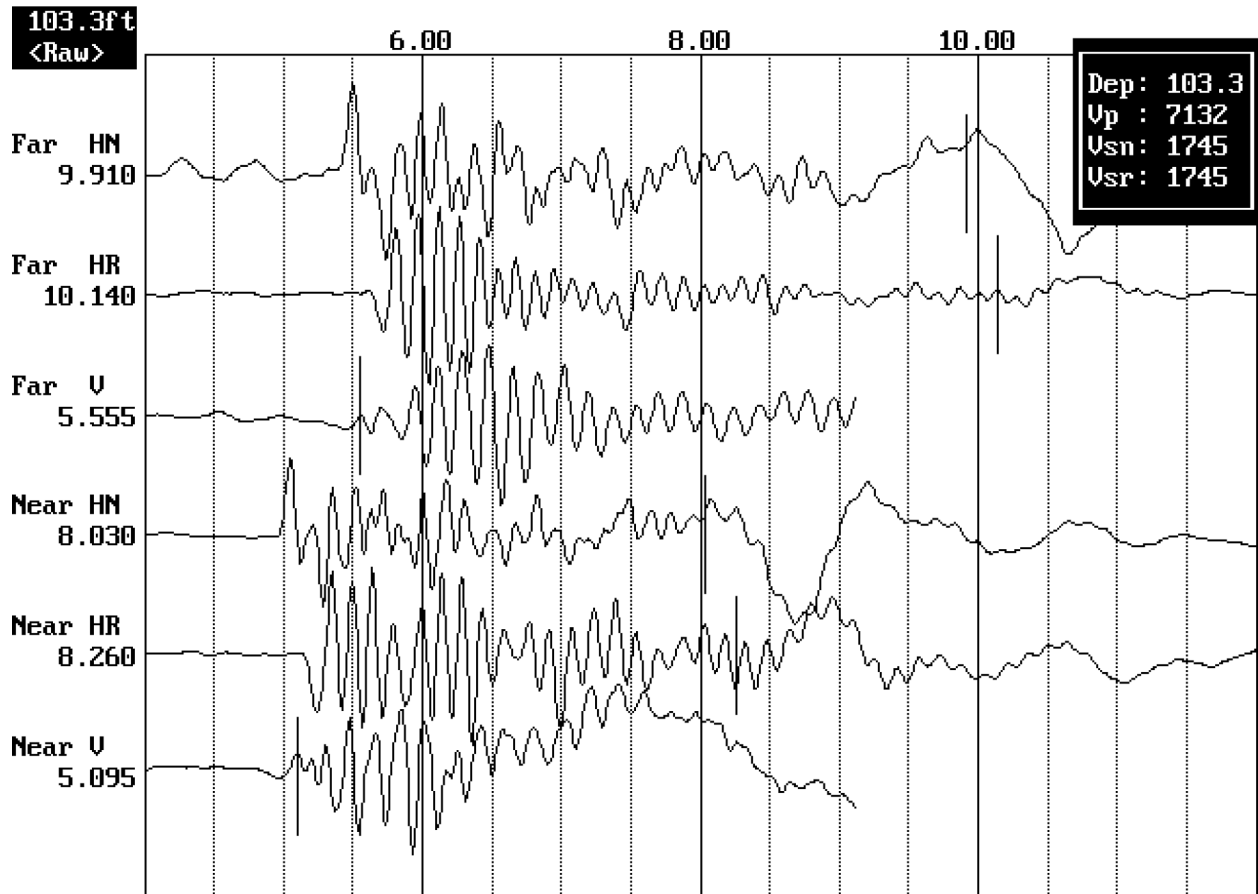


Figure 3. Example of unfiltered suspension record

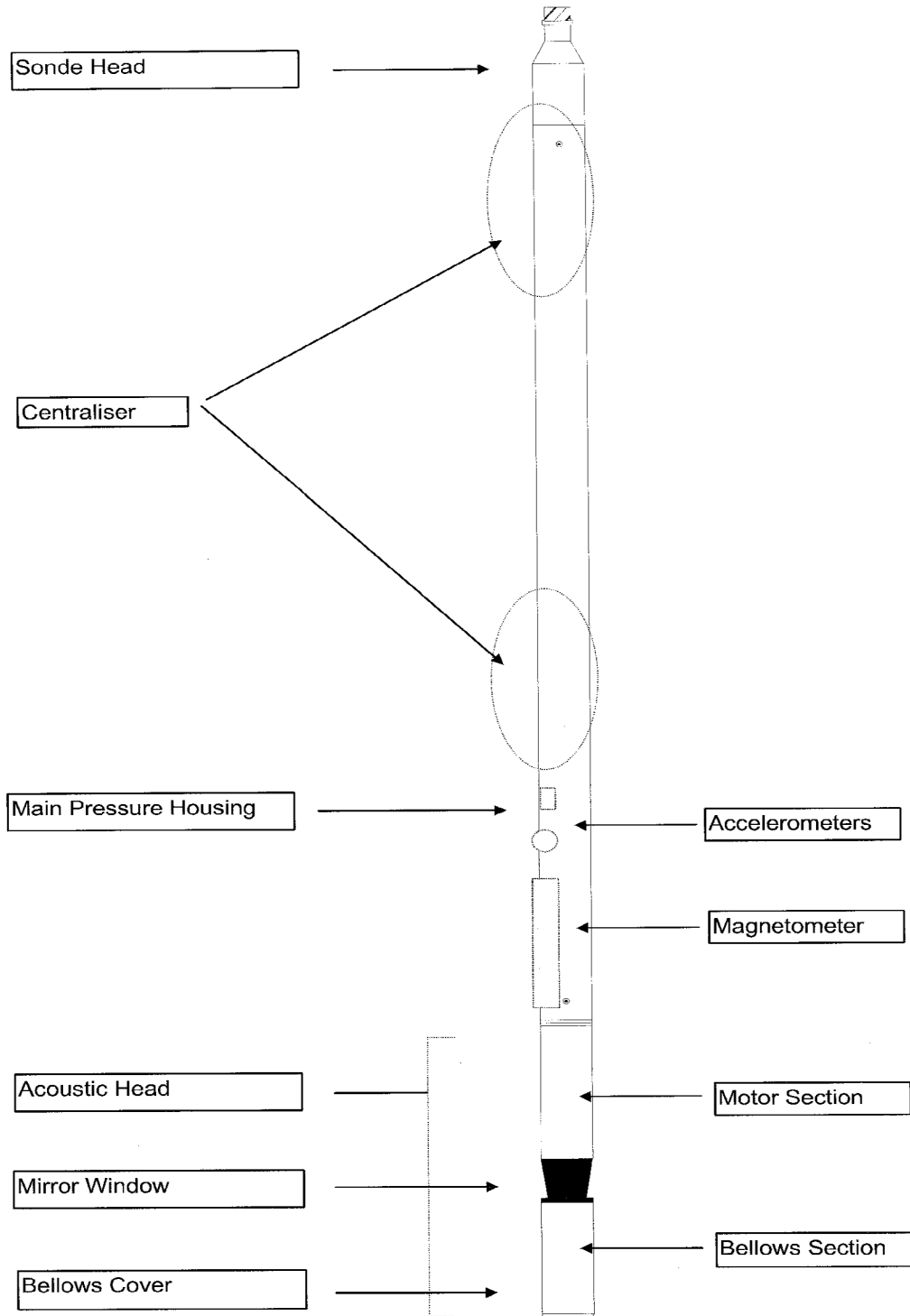


Figure 4: Concept illustration of televiwer probe

Deviated borehole in orthographic projection, viewed from N42

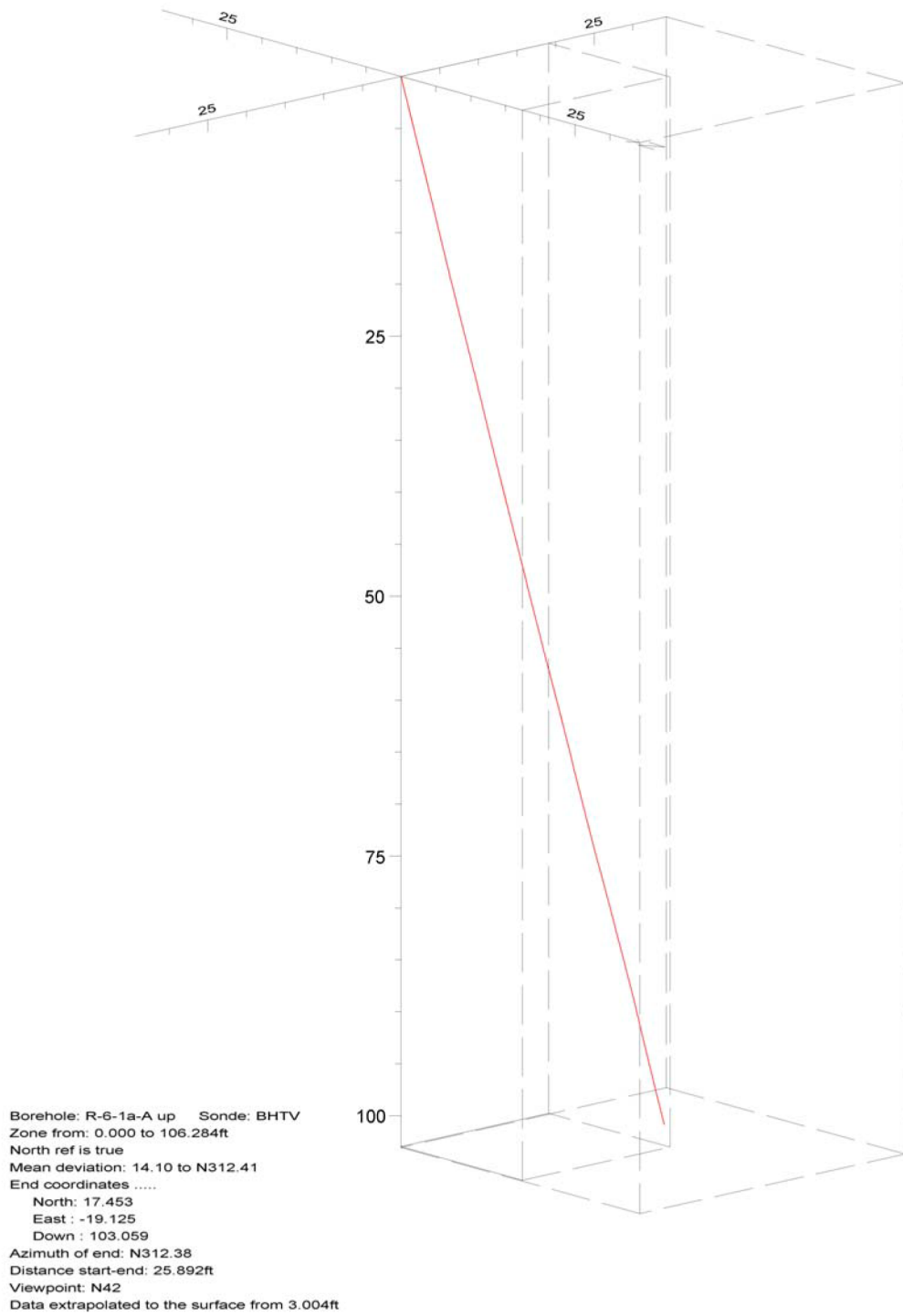


Figure 5. Boring R-6-1a-A, Up Deviation Projection (dimensions in feet)

TURKEY POINT 6&7 SITE BOREHOLE R-6-1b  
Receiver to Receiver  $V_s$  and  $V_p$  Analysis

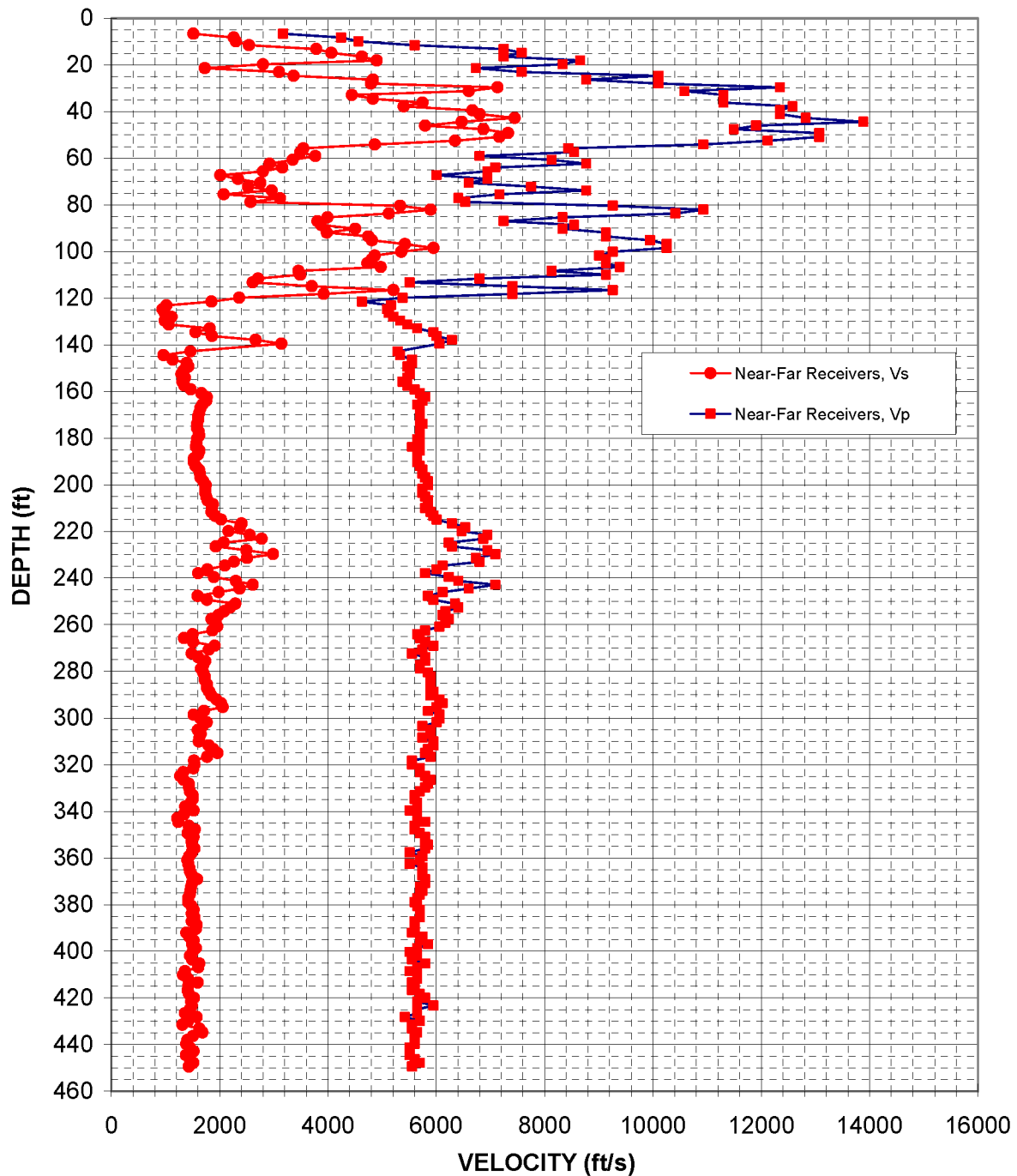


Figure 6: Boring R-6-1b Suspension R1-R2 P- and  $S_H$ -wave velocities

Table 5. Boring R-6-1b, Suspension R1-R2 depths and P- and S<sub>H</sub>-wave velocities

**Summary of Compressional Wave Velocity, Shear Wave Velocity, and Poisson's Ratio  
Based on Receiver-to-Receiver Travel Time Data - Borehole R-6-1b**

American Units				Metric Units			
Depth at Midpoint Between Receivers	Velocity		Poisson's Ratio	Depth at Midpoint Between Receivers	Velocity		Poisson's Ratio
	V <sub>s</sub>	V <sub>p</sub>			V <sub>s</sub>	V <sub>p</sub>	
(ft)	(ft/s)	(ft/s)		(m)	(m/s)	(m/s)	
6.6	1520	3170	0.35	2.0	460	970	0.35
8.2	2260	4250	0.30	2.5	690	1290	0.30
9.8	2300	4570	0.33	3.0	700	1390	0.33
11.5	2540	5600	0.37	3.5	780	1710	0.37
13.1	3790	7250	0.31	4.0	1150	2210	0.31
14.8	4070	7580	0.30	4.5	1240	2310	0.30
16.4	4630	7250	0.16	5.0	1410	2210	0.16
18.0	4900	8660	0.26	5.5	1490	2640	0.26
19.7	2800	8330	0.44	6.0	850	2540	0.44
21.3	1730	6730	0.46	6.5	530	2050	0.46
23.0	3100	7580	0.40	7.0	950	2310	0.40
24.6	3370	10100	0.44	7.5	1030	3080	0.44
26.3	4830	8770	0.28	8.0	1470	2670	0.28
27.9	4800	10100	0.35	8.5	1460	3080	0.35
29.5	7130	12350	0.25	9.0	2170	3760	0.25
31.2	6600	10580	0.18	9.5	2010	3230	0.18
32.8	4440	11300	0.41	10.0	1350	3440	0.41
34.5	4830	11300	0.39	10.5	1470	3440	0.39
36.1	5750	11300	0.33	11.0	1750	3440	0.33
37.7	5400	12580	0.39	11.5	1650	3830	0.39
39.4	6670	12350	0.29	12.0	2030	3760	0.29
41.0	6800	12350	0.28	12.5	2070	3760	0.28
42.7	7450	12820	0.25	13.0	2270	3910	0.25
44.3	6470	13890	0.36	13.5	1970	4230	0.36
45.9	5800	11900	0.34	14.0	1770	3630	0.34
47.6	6870	11490	0.22	14.5	2090	3500	0.22
49.2	7330	13070	0.27	15.0	2230	3980	0.27
50.9	7170	13070	0.28	15.5	2180	3980	0.28
52.5	6350	12120	0.31	16.0	1940	3690	0.31
54.1	4870	10930	0.38	16.5	1480	3330	0.38
55.8	3550	8440	0.39	17.0	1080	2570	0.39
57.4	3490	8550	0.40	17.5	1060	2610	0.40
59.1	3770	6800	0.28	18.0	1150	2070	0.28
60.7	3350	8130	0.40	18.5	1020	2480	0.40
62.3	2920	8770	0.44	19.0	890	2670	0.44
64.0	3160	7090	0.38	19.5	960	2160	0.38
65.6	2800	6940	0.40	20.0	850	2120	0.40

**Summary of Compressional Wave Velocity, Shear Wave Velocity, and Poisson's Ratio  
Based on Receiver-to-Receiver Travel Time Data - Borehole R-6-1b**

American Units			
Depth at Midpoint Between Receivers	Velocity		Poisson's Ratio
	V <sub>s</sub>	V <sub>p</sub>	
(ft)	(ft/s)	(ft/s)	
67.3	2010	6010	0.44
68.9	2340	6940	0.44
70.5	2750	6600	0.39
72.2	2530	7750	0.44
73.8	2960	8770	0.44
75.5	2080	7170	0.45
77.1	3120	6410	0.35
78.7	2570	6540	0.41
80.4	5330	9260	0.25
82.0	5900	10930	0.29
83.7	5130	10420	0.34
85.3	3990	8330	0.35
86.9	3810	7250	0.31
88.6	3880	8550	0.37
90.2	4500	8330	0.29
91.9	3980	9130	0.38
93.5	4740	9130	0.32
95.1	4810	9950	0.35
96.8	5420	10260	0.31
98.4	5950	10260	0.25
100.1	5350	9260	0.25
101.7	4870	9010	0.29
103.4	4810	9130	0.31
105.0	4730	9130	0.32
106.6	4980	9390	0.30
108.3	3450	8130	0.39
109.9	3490	9130	0.41
111.6	2710	6800	0.41
113.2	2610	5510	0.35
114.8	3700	7410	0.33
116.5	5210	9260	0.27
118.1	3920	7410	0.31
119.8	2360	5380	0.38
121.4	1850	4630	0.40
123.0	1020	5170	0.48
124.7	950	5090	0.48
126.3	990	5130	0.48
128.0	1110	5210	0.48
129.6	990	5330	0.48

Metric Units			
Depth at Midpoint Between Receivers	Velocity		Poisson's Ratio
	V <sub>s</sub>	V <sub>p</sub>	
(m)	(m/s)	(m/s)	
20.5	610	1830	0.44
21.0	710	2120	0.44
21.5	840	2010	0.39
22.0	770	2360	0.44
22.5	900	2670	0.44
23.0	630	2180	0.45
23.5	950	1950	0.35
24.0	780	1990	0.41
24.5	1630	2820	0.25
25.0	1800	3330	0.29
25.5	1560	3180	0.34
26.0	1220	2540	0.35
26.5	1160	2210	0.31
27.0	1180	2610	0.37
27.5	1370	2540	0.29
28.0	1210	2780	0.38
28.5	1450	2780	0.32
29.0	1470	3030	0.35
29.5	1650	3130	0.31
30.0	1810	3130	0.25
30.5	1630	2820	0.25
31.0	1480	2750	0.29
31.5	1470	2780	0.31
32.0	1440	2780	0.32
32.5	1520	2860	0.30
33.0	1050	2480	0.39
33.5	1060	2780	0.41
34.0	830	2070	0.41
34.5	800	1680	0.35
35.0	1130	2260	0.33
35.5	1590	2820	0.27
36.0	1200	2260	0.31
36.5	720	1640	0.38
37.0	560	1410	0.40
37.5	310	1580	0.48
38.0	290	1550	0.48
38.5	300	1560	0.48
39.0	340	1590	0.48
39.5	300	1630	0.48

**Summary of Compressional Wave Velocity, Shear Wave Velocity, and Poisson's Ratio  
Based on Receiver-to-Receiver Travel Time Data - Borehole R-6-1b**

American Units				Metric Units			
Depth at Midpoint Between Receivers	Velocity		Poisson's Ratio	Depth at Midpoint Between Receivers	Velocity		Poisson's Ratio
	V <sub>s</sub>	V <sub>p</sub>			V <sub>s</sub>	V <sub>p</sub>	
(ft)	(ft/s)	(ft/s)		(m)	(m/s)	(m/s)	
131.2	1060	5460	0.48	40.0	320	1670	0.48
132.9	1820	5650	0.44	40.5	560	1720	0.44
134.5	1560	5950	0.46	41.0	470	1810	0.46
136.2	1860	6010	0.45	41.5	570	1830	0.45
137.8	2670	6290	0.39	42.0	810	1920	0.39
139.4	3140	6060	0.32	42.5	960	1850	0.32
142.7	1460	5290	0.46	43.5	450	1610	0.46
144.4	970	5330	0.48	44.0	290	1630	0.48
146.3	1130	5560	0.48	44.6	350	1690	0.48
147.6	1390	5560	0.47	45.0	430	1690	0.47
149.3	1420	5460	0.46	45.5	430	1670	0.46
150.9	1340	5510	0.47	46.0	410	1680	0.47
152.6	1300	5510	0.47	46.5	400	1680	0.47
154.2	1360	5460	0.47	47.0	410	1670	0.47
155.8	1310	5380	0.47	47.5	400	1640	0.47
157.5	1350	5460	0.47	48.0	410	1670	0.47
159.1	1470	5600	0.46	48.5	450	1710	0.46
160.8	1670	5700	0.45	49.0	510	1740	0.45
162.4	1760	5800	0.45	49.5	540	1770	0.45
164.0	1750	5750	0.45	50.0	530	1750	0.45
165.7	1680	5650	0.45	50.5	510	1720	0.45
167.3	1640	5700	0.45	51.0	500	1740	0.45
169.0	1630	5700	0.46	51.5	500	1740	0.46
170.6	1600	5700	0.46	52.0	490	1740	0.46
172.2	1600	5700	0.46	52.5	490	1740	0.46
173.9	1590	5750	0.46	53.0	480	1750	0.46
175.5	1580	5700	0.46	53.5	480	1740	0.46
177.2	1610	5700	0.46	54.0	490	1740	0.46
178.8	1630	5700	0.46	54.5	500	1740	0.46
180.5	1580	5650	0.46	55.0	480	1720	0.46
182.1	1580	5700	0.46	55.5	480	1740	0.46
183.7	1560	5560	0.46	56.0	480	1690	0.46
185.4	1630	5700	0.46	56.5	500	1740	0.46
187.0	1600	5650	0.46	57.0	490	1720	0.46
188.7	1530	5650	0.46	57.5	470	1720	0.46
190.3	1530	5650	0.46	58.0	460	1720	0.46
191.9	1550	5700	0.46	58.5	470	1740	0.46
193.6	1620	5750	0.46	59.0	490	1750	0.46
195.2	1640	5750	0.46	59.5	500	1750	0.46

**Summary of Compressional Wave Velocity, Shear Wave Velocity, and Poisson's Ratio  
Based on Receiver-to-Receiver Travel Time Data - Borehole R-6-1b**

American Units			
Depth at Midpoint Between Receivers	Velocity		Poisson's Ratio
	V <sub>s</sub>	V <sub>p</sub>	
(ft)	(ft/s)	(ft/s)	
196.9	1650	5800	0.46
198.5	1700	5850	0.45
200.1	1750	5850	0.45
201.8	1740	5750	0.45
203.4	1740	5750	0.45
205.1	1750	5800	0.45
206.7	1780	5850	0.45
208.3	1880	5850	0.44
210.0	1860	5800	0.44
211.6	1850	5900	0.45
213.3	1920	5950	0.44
214.9	2030	6010	0.44
216.5	2410	6290	0.41
218.2	2380	6540	0.42
219.8	2160	6470	0.44
221.5	2550	6940	0.42
223.1	2780	6870	0.40
224.7	2080	6230	0.44
226.4	1930	6290	0.45
228.0	2500	6940	0.43
229.7	2990	7090	0.39
231.3	2510	6730	0.42
232.9	2270	6800	0.44
234.6	2100	6120	0.43
236.2	1780	6010	0.45
237.9	1610	5800	0.46
239.5	1890	6230	0.45
241.1	2300	6410	0.43
242.8	2610	7090	0.42
244.4	2370	6600	0.43
246.1	1980	6120	0.44
247.7	1590	5850	0.46
249.3	1770	5950	0.45
251.0	2290	6350	0.43
252.6	2190	6410	0.43
254.3	2080	6170	0.44
255.9	1980	6120	0.44
257.6	1850	6230	0.45
259.2	1930	6170	0.45

Metric Units			
Depth at Midpoint Between Receivers	Velocity		Poisson's Ratio
	V <sub>s</sub>	V <sub>p</sub>	
(m)	(m/s)	(m/s)	
60.0	500	1770	0.46
60.5	520	1780	0.45
61.0	530	1780	0.45
61.5	530	1750	0.45
62.0	530	1750	0.45
62.5	530	1770	0.45
63.0	540	1780	0.45
63.5	570	1780	0.44
64.0	570	1770	0.44
64.5	560	1800	0.45
65.0	580	1810	0.44
65.5	620	1830	0.44
66.0	730	1920	0.41
66.5	730	1990	0.42
67.0	660	1970	0.44
67.5	780	2120	0.42
68.0	850	2090	0.40
68.5	630	1900	0.44
69.0	590	1920	0.45
69.5	760	2120	0.43
70.0	910	2160	0.39
70.5	760	2050	0.42
71.0	690	2070	0.44
71.5	640	1860	0.43
72.0	540	1830	0.45
72.5	490	1770	0.46
73.0	580	1900	0.45
73.5	700	1950	0.43
74.0	800	2160	0.42
74.5	720	2010	0.43
75.0	600	1860	0.44
75.5	490	1780	0.46
76.0	540	1810	0.45
76.5	700	1940	0.43
77.0	670	1950	0.43
77.5	640	1880	0.44
78.0	600	1860	0.44
78.5	560	1900	0.45
79.0	590	1880	0.45

**Summary of Compressional Wave Velocity, Shear Wave Velocity, and Poisson's Ratio  
Based on Receiver-to-Receiver Travel Time Data - Borehole R-6-1b**

American Units			
Depth at Midpoint Between Receivers	Velocity		Poisson's Ratio
	V <sub>s</sub>	V <sub>p</sub>	
(ft)	(ft/s)	(ft/s)	
260.8	1960	6060	0.44
262.5	1870	5800	0.44
264.1	1500	5650	0.46
265.8	1340	5700	0.47
267.4	1510	5800	0.46
269.0	1910	5950	0.44
270.7	1800	5750	0.45
272.3	1480	5560	0.46
274.0	1600	5800	0.46
275.6	1740	5800	0.45
277.2	1700	5700	0.45
278.9	1660	5700	0.45
280.5	1700	5850	0.45
282.2	1730	5900	0.45
283.8	1730	5900	0.45
285.4	1770	5900	0.45
287.1	1770	5900	0.45
288.7	1810	5950	0.45
290.4	1850	5900	0.45
292.0	1940	6060	0.44
293.6	2030	6120	0.44
295.3	2060	6010	0.43
296.9	1710	5850	0.45
298.6	1520	6060	0.47
300.2	1650	6060	0.46
301.8	1760	6010	0.45
303.5	1690	5750	0.45
305.1	1600	5900	0.46
306.8	1650	5900	0.46
308.4	1630	5750	0.46
310.0	1620	5950	0.46
311.7	1800	5950	0.45
313.3	1890	5850	0.44
315.0	1960	5800	0.44
316.6	1770	5900	0.45
318.2	1530	5560	0.46
319.9	1540	5560	0.46
321.5	1520	5700	0.46
323.2	1330	5700	0.47

Metric Units			
Depth at Midpoint Between Receivers	Velocity		Poisson's Ratio
	V <sub>s</sub>	V <sub>p</sub>	
(m)	(m/s)	(m/s)	
79.5	600	1850	0.44
80.0	570	1770	0.44
80.5	460	1720	0.46
81.0	410	1740	0.47
81.5	460	1770	0.46
82.0	580	1810	0.44
82.5	550	1750	0.45
83.0	450	1690	0.46
83.5	490	1770	0.46
84.0	530	1770	0.45
84.5	520	1740	0.45
85.0	510	1740	0.45
85.5	520	1780	0.45
86.0	530	1800	0.45
86.5	530	1800	0.45
87.0	540	1800	0.45
87.5	540	1800	0.45
88.0	550	1810	0.45
88.5	560	1800	0.45
89.0	590	1850	0.44
89.5	620	1860	0.44
90.0	630	1830	0.43
90.5	520	1780	0.45
91.0	460	1850	0.47
91.5	500	1850	0.46
92.0	540	1830	0.45
92.5	510	1750	0.45
93.0	490	1800	0.46
93.5	500	1800	0.46
94.0	500	1750	0.46
94.5	490	1810	0.46
95.0	550	1810	0.45
95.5	580	1780	0.44
96.0	600	1770	0.44
96.5	540	1800	0.45
97.0	470	1690	0.46
97.5	470	1690	0.46
98.0	460	1740	0.46
98.5	410	1740	0.47

**Summary of Compressional Wave Velocity, Shear Wave Velocity, and Poisson's Ratio  
Based on Receiver-to-Receiver Travel Time Data - Borehole R-6-1b**

American Units			
Depth at Midpoint Between Receivers	Velocity		Poisson's Ratio
	V <sub>s</sub>	V <sub>p</sub>	
(ft)	(ft/s)	(ft/s)	
324.8	1270	5800	0.47
326.4	1330	5900	0.47
328.1	1430	5850	0.47
329.7	1440	5800	0.47
331.4	1450	5700	0.47
333.0	1500	5600	0.46
334.7	1510	5600	0.46
336.3	1470	5650	0.46
337.9	1370	5650	0.47
339.6	1520	5510	0.46
341.2	1340	5650	0.47
342.9	1220	5650	0.48
344.5	1240	5800	0.48
346.1	1430	5600	0.47
347.8	1540	5600	0.46
349.4	1410	5700	0.47
351.1	1520	5800	0.46
352.7	1480	5800	0.47
354.3	1490	5850	0.47
356.0	1540	5800	0.46
357.6	1490	5510	0.46
359.3	1440	5750	0.47
360.9	1410	5700	0.47
362.5	1420	5510	0.46
364.2	1440	5750	0.47
365.8	1460	5750	0.47
367.5	1490	5750	0.46
369.1	1590	5800	0.46
370.7	1490	5800	0.46
372.4	1470	5700	0.46
374.0	1460	5750	0.47
375.7	1450	5700	0.47
377.3	1420	5650	0.47
378.9	1420	5600	0.47
380.6	1480	5650	0.46
382.2	1520	5700	0.46
383.9	1490	5700	0.46
385.5	1540	5700	0.46
387.1	1490	5600	0.46

Metric Units			
Depth at Midpoint Between Receivers	Velocity		Poisson's Ratio
	V <sub>s</sub>	V <sub>p</sub>	
(m)	(m/s)	(m/s)	
99.0	390	1770	0.47
99.5	410	1800	0.47
100.0	440	1780	0.47
100.5	440	1770	0.47
101.0	440	1740	0.47
101.5	460	1710	0.46
102.0	460	1710	0.46
102.5	450	1720	0.46
103.0	420	1720	0.47
103.5	460	1680	0.46
104.0	410	1720	0.47
104.5	370	1720	0.48
105.0	380	1770	0.48
105.5	440	1710	0.47
106.0	470	1710	0.46
106.5	430	1740	0.47
107.0	460	1770	0.46
107.5	450	1770	0.47
108.0	460	1780	0.47
108.5	470	1770	0.46
109.0	450	1680	0.46
109.5	440	1750	0.47
110.0	430	1740	0.47
110.5	430	1680	0.46
111.0	440	1750	0.47
111.5	440	1750	0.47
112.0	450	1750	0.46
112.5	480	1770	0.46
113.0	460	1770	0.46
113.5	450	1740	0.46
114.0	450	1750	0.47
114.5	440	1740	0.47
115.0	430	1720	0.47
115.5	430	1710	0.47
116.0	450	1720	0.46
116.5	460	1740	0.46
117.0	450	1740	0.46
117.5	470	1740	0.46
118.0	450	1710	0.46

**Summary of Compressional Wave Velocity, Shear Wave Velocity, and Poisson's Ratio  
Based on Receiver-to-Receiver Travel Time Data - Borehole R-6-1b**

American Units			
Depth at Midpoint Between Receivers	Velocity		Poisson's Ratio
	V <sub>s</sub>	V <sub>p</sub>	
(ft)	(ft/s)	(ft/s)	
388.8	1580	5600	0.46
390.4	1560	5600	0.46
392.1	1390	5560	0.47
393.7	1440	5750	0.47
395.3	1520	5700	0.46
397.0	1490	5850	0.47
398.6	1560	5650	0.46
400.3	1500	5510	0.46
401.9	1460	5650	0.46
403.5	1490	5560	0.46
405.2	1630	5800	0.46
406.8	1610	5650	0.46
408.5	1360	5510	0.47
410.1	1330	5650	0.47
411.8	1420	5650	0.47
413.4	1590	5560	0.46
415.0	1420	5600	0.47
416.7	1410	5560	0.47
418.3	1440	5700	0.47
420.0	1530	5800	0.46
421.6	1470	5650	0.46
423.2	1490	5950	0.47
424.9	1450	5650	0.46
426.5	1360	5650	0.47
428.2	1580	5420	0.45
429.8	1420	5700	0.47
431.4	1310	5560	0.47
433.1	1630	5560	0.45
434.7	1680	5650	0.45
436.4	1510	5600	0.46
438.0	1410	5600	0.47
439.6	1380	5600	0.47
441.3	1460	5510	0.46
442.9	1520	5510	0.46
444.6	1380	5510	0.47
446.2	1450	5600	0.46
447.8	1520	5700	0.46
449.5	1430	5560	0.46

Metric Units			
Depth at Midpoint Between Receivers	Velocity		Poisson's Ratio
	V <sub>s</sub>	V <sub>p</sub>	
(m)	(m/s)	(m/s)	
118.5	480	1710	0.46
119.0	480	1710	0.46
119.5	420	1690	0.47
120.0	440	1750	0.47
120.5	460	1740	0.46
121.0	460	1780	0.47
121.5	480	1720	0.46
122.0	460	1680	0.46
122.5	440	1720	0.46
123.0	460	1690	0.46
123.5	500	1770	0.46
124.0	490	1720	0.46
124.5	410	1680	0.47
125.0	400	1720	0.47
125.5	430	1720	0.47
126.0	490	1690	0.46
126.5	430	1710	0.47
127.0	430	1690	0.47
127.5	440	1740	0.47
128.0	470	1770	0.46
128.5	450	1720	0.46
129.0	450	1810	0.47
129.5	440	1720	0.46
130.0	410	1720	0.47
130.5	480	1650	0.45
131.0	430	1740	0.47
131.5	400	1690	0.47
132.0	500	1690	0.45
132.5	510	1720	0.45
133.0	460	1710	0.46
133.5	430	1710	0.47
134.0	420	1710	0.47
134.5	440	1680	0.46
135.0	460	1680	0.46
135.5	420	1680	0.47
136.0	440	1710	0.46
136.5	460	1740	0.46
137.0	440	1690	0.46

Table 6. Boring R-6-1b, Structure depth, dip azimuth, dip and structure description

Depth (feet)	Dip azimuth	Dip	Structure description
15.7	N203	34	Primary-structure Planar Weathered Bedding
17.6	N354	30	Primary-structure Planar Weathered Bedding
18.6	N307	50	Primary-structure Planar Weathered Bedding
26.1	N227	24	Primary-structure Planar Weathered Bedding
26.4	N184	7	Primary-structure Planar Weathered Bedding
30.5	N256	29	Primary-structure Planar Weathered Bedding
32.2	N179	24	Primary-structure Planar Weathered Bedding
33.0	N344	48	Primary-structure Planar Weathered Bedding
37.2	N115	77	Primary-structure Planar Weathered Bedding
46.7	N274	46	Primary-structure Planar Weathered Bedding
49.6	N188	14	Fracture Planar Hairline-fracture
57.4	N238	24	Primary-structure Planar Weathered Bedding
59.8	N229	5	Primary-structure Planar Weathered Bedding
61.2	N018	9	Fracture Planar Open-fracture
65.9	N188	18	Primary-structure Planar Weathered Bedding
77.2	N174	28	Primary-structure Planar Weathered Bedding
79.7	N142	52	Primary-structure Planar Weathered Bedding
98.2	N303	38	Primary-structure Planar Weathered Bedding
112.5	N277	36	Primary-structure Planar Weathered Bedding
364.3	N097	32	Primary-structure Planar Weathered Bedding
446.9	N336	15	Primary-structure Planar Weathered Bedding
455.4	N308	33	Primary-structure Planar Weathered Bedding

Deviated borehole in orthographic projection, viewed from N101

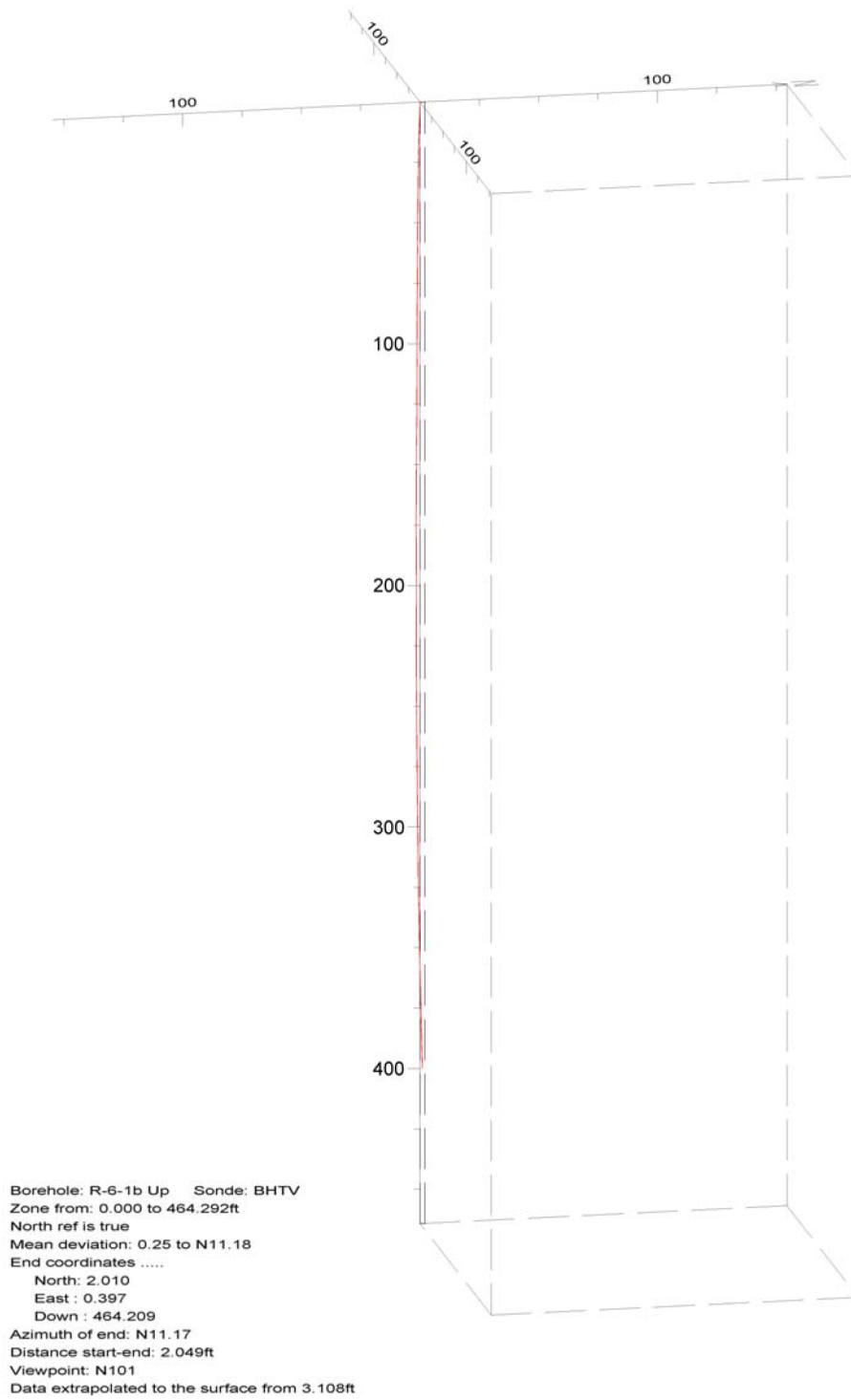


Figure 7. Boring R-6-1b, Up Deviation Projection (dimensions in feet)

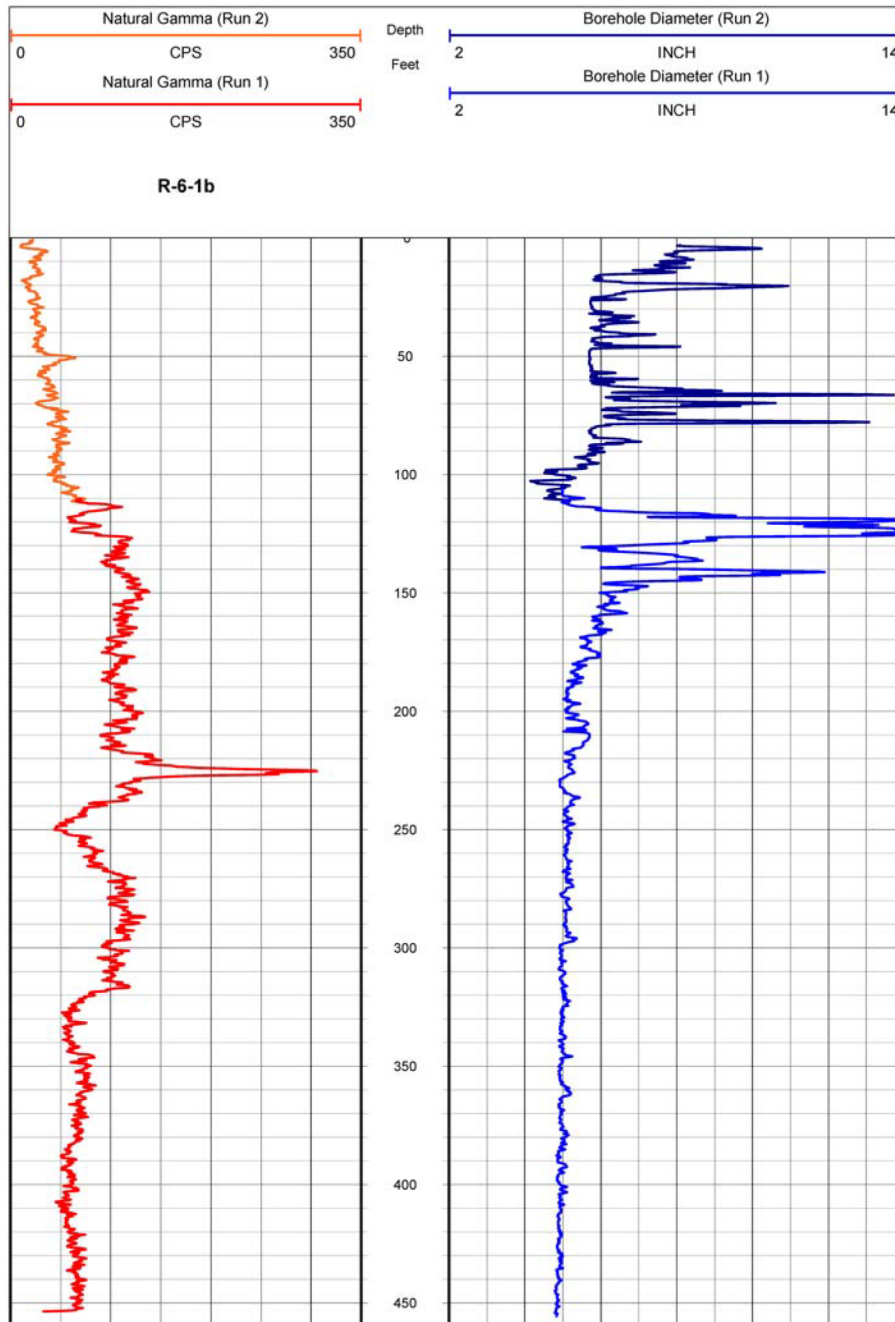


Figure 8. Boring R-6-1b, Caliper and Natural gamma logs

TURKEY POINT 6&7 SITE BOREHOLE R-7-1  
Receiver to Receiver  $V_s$  and  $V_p$  Analysis

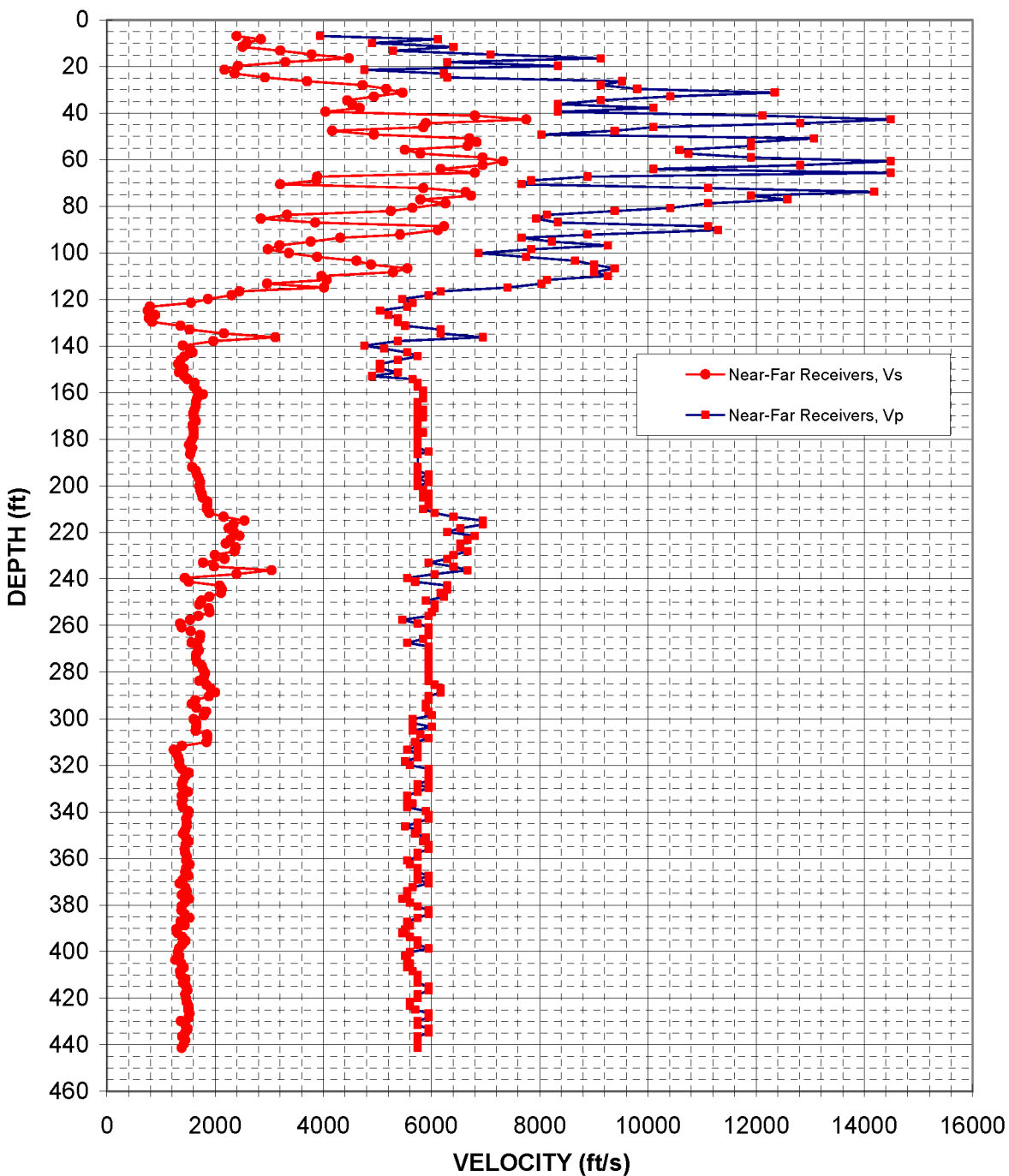


Figure 9: Boring R-7-1, Suspension R1-R2 P- and  $S_H$ -wave velocities

Table 7. Boring R-7-1, Suspension R1-R2 depths and P- and S<sub>H</sub>-wave velocities

**Summary of Compressional Wave Velocity, Shear Wave Velocity, and Poisson's Ratio  
Based on Receiver-to-Receiver Travel Time Data - Borehole R-7-1**

American Units				Metric Units			
Depth at Midpoint Between Receivers	Velocity		Poisson's Ratio	Depth at Midpoint Between Receivers	Velocity		Poisson's Ratio
	V <sub>s</sub>	V <sub>p</sub>			V <sub>s</sub>	V <sub>p</sub>	
(ft)	(ft/s)	(ft/s)		(m)	(m/s)	(m/s)	
6.9	2400	3940	0.21	2.1	730	1200	0.21
8.2	2850	6120	0.36	2.5	870	1860	0.36
9.8	2580	4900	0.31	3.0	790	1490	0.31
11.5	2510	6410	0.41	3.5	760	1950	0.41
13.1	3210	5290	0.21	4.0	980	1610	0.21
14.8	3790	7090	0.30	4.5	1150	2160	0.30
16.4	4470	9130	0.34	5.0	1360	2780	0.34
18.0	3300	6290	0.31	5.5	1010	1920	0.31
19.7	2420	8330	0.45	6.0	740	2540	0.45
21.3	2180	4760	0.37	6.5	660	1450	0.37
23.0	2360	6230	0.42	7.0	720	1900	0.42
24.6	2920	6290	0.36	7.5	890	1920	0.36
26.3	3700	9520	0.41	8.0	1130	2900	0.41
27.9	4730	9130	0.32	8.5	1440	2780	0.32
29.5	5170	9800	0.31	9.0	1580	2990	0.31
31.2	5460	12350	0.38	9.5	1670	3760	0.38
32.8	4940	10420	0.36	10.0	1510	3180	0.36
34.5	4440	9130	0.34	10.5	1350	2780	0.34
36.1	4540	8330	0.29	11.0	1380	2540	0.29
37.7	4680	10100	0.36	11.5	1430	3080	0.36
39.4	4040	8330	0.35	12.0	1230	2540	0.35
41.0	6800	12120	0.27	12.5	2070	3690	0.27
42.7	7750	14490	0.30	13.0	2360	4420	0.30
44.3	5900	12820	0.37	13.5	1800	3910	0.37
45.9	5850	10100	0.25	14.0	1780	3080	0.25
47.6	4170	9390	0.38	14.5	1270	2860	0.38
49.2	4940	8030	0.20	15.0	1510	2450	0.20
50.9	6700	13070	0.32	15.5	2040	3980	0.32
52.5	6840	11900	0.25	16.0	2080	3630	0.25
54.1	6670	11900	0.27	16.5	2030	3630	0.27
55.8	5510	10580	0.31	17.0	1680	3230	0.31
57.4	5800	10750	0.30	17.5	1770	3280	0.30
59.1	6940	11900	0.24	18.0	2120	3630	0.24
60.7	7330	14490	0.33	18.5	2230	4420	0.33
62.3	6940	12820	0.29	19.0	2120	3910	0.29
64.0	6170	10100	0.20	19.5	1880	3080	0.20
65.6	6800	14490	0.36	20.0	2070	4420	0.36

**Summary of Compressional Wave Velocity, Shear Wave Velocity, and Poisson's Ratio  
Based on Receiver-to-Receiver Travel Time Data - Borehole R-7-1**

American Units				Metric Units			
Depth at Midpoint Between Receivers	Velocity		Poisson's Ratio	Depth at Midpoint Between Receivers	Velocity		Poisson's Ratio
	V <sub>s</sub>	V <sub>p</sub>			V <sub>s</sub>	V <sub>p</sub>	
(ft)	(ft/s)	(ft/s)		(m)	(m/s)	(m/s)	
67.3	3890	8890	0.38	20.5	1180	2710	0.38
68.9	3880	7840	0.34	21.0	1180	2390	0.34
70.5	3210	7660	0.39	21.5	980	2340	0.39
72.2	5850	11110	0.31	22.0	1780	3390	0.31
73.8	6630	14180	0.36	22.5	2020	4320	0.36
75.5	6730	11900	0.26	23.0	2050	3630	0.26
77.1	5800	12580	0.37	23.5	1770	3830	0.37
78.7	6260	11110	0.27	24.0	1910	3390	0.27
80.7	5650	10420	0.29	24.6	1720	3180	0.29
82.0	5250	9390	0.27	25.0	1600	2860	0.27
83.7	3330	8130	0.40	25.5	1020	2480	0.40
85.3	2850	7940	0.43	26.0	870	2420	0.43
86.9	3850	8330	0.36	26.5	1170	2540	0.36
88.6	6230	11110	0.27	27.0	1900	3390	0.27
90.2	6120	11300	0.29	27.5	1860	3440	0.29
92.2	5420	8890	0.20	28.1	1650	2710	0.20
93.5	4310	7660	0.27	28.5	1320	2340	0.27
95.1	3770	8230	0.37	29.0	1150	2510	0.37
96.8	3190	9260	0.43	29.5	970	2820	0.43
98.4	2980	7840	0.42	30.0	910	2390	0.42
100.1	3370	6870	0.34	30.5	1030	2090	0.34
101.7	3890	7750	0.33	31.0	1180	2360	0.33
103.4	4610	8660	0.30	31.5	1410	2640	0.30
105.0	4880	9010	0.29	32.0	1490	2750	0.29
106.6	5560	9390	0.23	32.5	1690	2860	0.23
108.3	5290	9010	0.24	33.0	1610	2750	0.24
109.9	3970	9260	0.39	33.5	1210	2820	0.39
111.6	4070	8130	0.33	34.0	1240	2480	0.33
113.2	2960	8030	0.42	34.5	900	2450	0.42
114.8	4020	7410	0.29	35.0	1220	2260	0.29
116.5	2450	6170	0.41	35.5	750	1880	0.41
118.1	2310	5950	0.41	36.0	700	1810	0.41
119.8	1870	5460	0.43	36.5	570	1670	0.43
121.4	1560	5650	0.46	37.0	470	1720	0.46
123.0	800	5560	0.49	37.5	240	1690	0.49
124.7	760	5050	0.49	38.0	230	1540	0.49
126.6	890	5210	0.48	38.6	270	1590	0.48
128.0	780	5380	0.49	39.0	240	1640	0.49
129.6	840	5380	0.49	39.5	260	1640	0.49

**Summary of Compressional Wave Velocity, Shear Wave Velocity, and Poisson's Ratio  
Based on Receiver-to-Receiver Travel Time Data - Borehole R-7-1**

American Units			
Depth at Midpoint Between Receivers	Velocity		Poisson's Ratio
	V <sub>s</sub>	V <sub>p</sub>	
(ft)	(ft/s)	(ft/s)	
131.2	1360	5510	0.47
132.9	1530	6170	0.47
134.5	2160	6170	0.43
136.2	3120	6940	0.37
137.8	1970	5380	0.42
139.8	1410	4760	0.45
141.1	1530	5130	0.45
142.7	1590	5560	0.46
144.4	1440	5750	0.47
146.0	1360	5380	0.47
147.6	1320	5050	0.46
149.6	1420	5050	0.46
151.3	1330	5380	0.47
152.9	1430	4900	0.45
154.2	1490	5650	0.46
155.8	1620	5750	0.46
157.5	1610	5750	0.46
159.1	1670	5850	0.46
160.8	1780	5850	0.45
162.4	1670	5850	0.46
164.0	1650	5750	0.46
165.7	1650	5750	0.46
167.3	1620	5850	0.46
169.0	1590	5750	0.46
170.6	1610	5850	0.46
172.2	1650	5750	0.46
173.9	1590	5750	0.46
175.5	1600	5750	0.46
177.2	1610	5850	0.46
178.8	1610	5750	0.46
180.5	1570	5750	0.46
182.4	1520	5750	0.46
183.7	1580	5750	0.46
185.4	1550	5950	0.46
186.4	1540	5750	0.46
191.9	1580	5750	0.46
193.6	1650	5750	0.46
195.2	1670	5950	0.46
196.9	1700	5750	0.45

Metric Units			
Depth at Midpoint Between Receivers	Velocity		Poisson's Ratio
	V <sub>s</sub>	V <sub>p</sub>	
(m)	(m/s)	(m/s)	
40.0	410	1680	0.47
40.5	470	1880	0.47
41.0	660	1880	0.43
41.5	950	2120	0.37
42.0	600	1640	0.42
42.6	430	1450	0.45
43.0	470	1560	0.45
43.5	480	1690	0.46
44.0	440	1750	0.47
44.5	410	1640	0.47
45.0	400	1540	0.46
45.6	430	1540	0.46
46.1	410	1640	0.47
46.6	440	1490	0.45
47.0	450	1720	0.46
47.5	490	1750	0.46
48.0	490	1750	0.46
48.5	510	1780	0.46
49.0	540	1780	0.45
49.5	510	1780	0.46
50.0	500	1750	0.46
50.5	500	1750	0.46
51.0	490	1780	0.46
51.5	490	1750	0.46
52.0	490	1780	0.46
52.5	500	1750	0.46
53.0	480	1750	0.46
53.5	490	1750	0.46
54.0	490	1780	0.46
54.5	490	1750	0.46
55.0	480	1750	0.46
55.6	460	1750	0.46
56.0	480	1750	0.46
56.5	470	1810	0.46
56.8	470	1750	0.46
58.5	480	1750	0.46
59.0	500	1750	0.46
59.5	510	1810	0.46
60.0	520	1750	0.45